UC San Diego
UC San Diego Previously Published Works

Title

Cover Image, Volume 72, Issue 5

Permalink

Journal

ISSN

Authors

Martellucci, Stefano

Flütsch, Andreas

Carter, Mark

et al.

Publication Date

DOI

Copyright Information

Peer reviewed

GLIA

WILEY

RESEARCH ARTICLE

Axon-derived PACSIN1 binds to the Schwann cell survival receptor, LRP1, and transactivates TrkC to promote gliatrophic activities

Stefano Martellucci[1] ![ORCID] | Andreas Flütsch[1] | Mark Carter[1] | Masaki Norimoto[1] | Donald Pizzo[2] | Elisabetta Mantuano[2] | Mahrou Sadri[1] | Zixuan Wang[1] | Daisy Chillin-Fuentes[3] | Sara Brin Rosenthal[3] | Pardis Azmoon[2] | Steven L. Gonias[2] | Wendy M. Campana[1,4,5] ![ORCID]

[1]Department of Anesthesiology, University of California San Diego, La Jolla, California, USA

[2]Department of Pathology, University of California San Diego, La Jolla, California, USA

[3]Center for Computational Biology & Bioinformatics, Altman Clinical & Translational Research Institute, University of California San Diego, La Jolla, California, USA

[4]Program in Neurosciences, University of California San Diego, La Jolla, California, USA

[5]Division of Research, San Diego VA Health Care System, San Diego, California, USA

Correspondence
Wendy M. Campana, Department of Anesthesiology, University of California San Diego, La Jolla, CA 92093, USA.
Email: wcampana@ucsd.edu

Abstract

Schwann cells (SCs) undergo phenotypic transformation and then orchestrate nerve repair following PNS injury. The ligands and receptors that activate and sustain SC transformation remain incompletely understood. Proteins released by injured axons represent important candidates for activating the SC Repair Program. The low-density lipoprotein receptor-related protein-1 (LRP1) is acutely up-regulated in SCs in response to injury, activating c-Jun, and promoting SC survival. To identify novel LRP1 ligands released in PNS injury, we applied a discovery-based approach in which extracellular proteins in the injured nerve were captured using Fc-fusion proteins containing the ligand-binding motifs of LRP1 (CCR2 and CCR4). An intracellular neuron-specific protein, Protein Kinase C and Casein Kinase Substrate in Neurons (PACSIN1) was identified and validated as an LRP1 ligand. Recombinant PACSIN1 activated c-Jun and ERK1/2 in cultured SCs. Silencing *Lrp1* or inhibiting the LRP1 cell-signaling co-receptor, the NMDA-R, blocked the effects of PACSIN1 on c-Jun and ERK1/2 phosphorylation. Intraneural injection of PACSIN1 into crush-injured sciatic nerves activated c-Jun in wild-type mice, but not in mice in which *Lrp1* is conditionally deleted in SCs. Transcriptome profiling of SCs revealed that PACSIN1 mediates gene expression events consistent with transformation to the repair phenotype. PACSIN1 promoted SC migration and viability following the TNFα challenge. When Src family kinases were pharmacologically inhibited or the receptor tyrosine kinase, TrkC, was genetically silenced or pharmacologically inhibited, PACSIN1 failed to induce cell signaling and prevent SC death. Collectively, these studies demonstrate that PACSIN1 is a novel axon-derived LRP1 ligand that activates SC repair signaling by transactivating TrkC.

KEYWORDS
axon glia interaction, cell signaling, injury-repair, LRP1, Schwann cells

1 | INTRODUCTION

Injury to the peripheral nervous system (PNS) triggers a transformation in Schwann cell (SC) gene expression and phenotype, referred to as activation of the SC Repair Program. This process is essential for Wallerian degeneration and successful functional nerve regeneration (Jessen & Mirsky, 2016; Lehmann & Höke, 2010). When activation of the SC Repair Program is compromised, for example in aged rodents or chronic denervation, the capacity for damaged axon regeneration is decreased (Jessen & Mirsky, 2019; Painter et al., 2014). After injury, SCs do not merely de-differentiate but transdifferentiate to a repair state, expressing a unique transcriptome that is distinct from other SCs including those involved in development (Jessen & Mirsky, 2016). The injury-induced transcription factor, c-Jun, plays a critical role in SC transformation to the repair phenotype (Arthur-Farraj et al., 2012). After nerve injury, c-Jun is increased in SCs for 1–2 weeks. When the gene encoding c-Jun is conditionally deleted in SCs, neuronal viability, axonal regeneration, and functional recovery after injury are severely compromised (Arthur-Farraj et al., 2012). Factors known to activate c-Jun in SCs include neuregulin (Syed et al., 2010) and NT-3 (Yamauchi et al., 2003). Although proteins released by injured nerves may function as important triggers of the SC repair phenotype, specific proteins released by injured axons that promote SC c-Jun activation have not been identified.

The low-density lipoprotein receptor-related protein 1 (LRP1) is an endocytic and cell-signaling receptor for over 100 structurally and functionally diverse ligands (Gonias & Campana, 2014; Strickland et al., 2002). A subset of LRP1 ligands initiate cell-signaling by engaging LRP1, together with coreceptors that may include the N-methyl-D-aspartate receptor (NMDA-R), Trk receptors, p75^{NTR}, and/or nonpathogenic cellular prion protein (Mantuano et al., 2013; Martin et al., 2008; Mattei et al., 2020; May et al., 2004; Shi et al., 2009; Stiles et al., 2013; Taylor & Hooper, 2007). The effects of LRP1-initiated cell-signaling are distinct in different cell types; however, many of the effects of LRP1 on cell physiology suggest a model in which LRP1 orchestrates the response to tissue injury (Gonias & Campana, 2014). This model may explain why LRP1 evolved to have a broad continuum of ligands and is supported by LC–MS/MS proteomics studies demonstrating that LRP1 ligands include intracellular proteins, released by cells in tissue injury (Fernandez-Castaneda et al., 2013).

In the uninjured peripheral nerve, SCs express low levels of LRP1; however, in response to PNS injury, SC LRP1 levels increase substantially (Campana et al., 2006). LRP1 promotes SC survival by activating the PI3K/Akt signaling pathway and by antagonizing the adaptive unfolded protein response (UPR) pathways (Mantuano et al., 2008; Mantuano et al., 2011). Ligand-binding to LRP1 in SCs also activates c-Jun and ERK1/2, which may support SC transformation into the repair phenotype (Flütsch et al., 2016; Mantuano et al., 2008), although an absolute requirement of LRP1 in generating the repair phenotype has not been demonstrated in vivo. LRP1 promotes cell migration, a key feature of the SC repair phenotype (Mantuano et al., 2008). Transgenic mice in which the gene encoding LRP1 (*Lrp1*) is deleted in nonmyelinating and myelinating SCs demonstrate

increased neuropathic pain after injury (Orita et al., 2013). This is associated with accelerated Wallerian degeneration, compromised axon regeneration, and loss of functional sensory nerve repair (Orita et al., 2013; Poplawski et al., 2018). Reduced expression of *Lrp1* may serve as a biomarker for diabetic peripheral neuropathy diagnosis and progression (El-Horany et al., 2019) and activation of LRP1 may improve painful peripheral neuropathy (Garcia-Fernandez et al., 2021; Wang et al., 2022).

The goal of the present study was to identify proteins released by injured peripheral nerves that may trigger LRP1-dependent cell signaling in support of the SC Repair Program. We applied a novel method to isolate proteins from the extracellular spaces of the sciatic nerve without lysing cells. LRP1 ligands were affinity-purified using fusion proteins that include the ligand-binding motifs in the LRP1 α-chain (Stiles et al., 2013; Strickland et al., 2002) and then, identified by LC–MS/MS. Validation studies confirmed that the intracellular protein, Protein Kinase C and Casein Kinase Substrate in Neurons (PACSIN1), is a neuronal LRP1 ligand capable of activating cell-signaling and gene expression in SCs. PACSIN1 is abundantly expressed in PNS neurons (Boll et al., 2020; Liu et al., 2012), but not by SCs. The response to PACSIN1 required LRP1 co-receptors, including the NMDA-R and TrkC. Previously, we identified TrkC as an LRP1 co-receptor in sensory neurons (Yoon et al., 2013), but not in SCs. We conclude that Trk receptors may function as LRP1 co-receptors in glia, in addition to neurons. Overall, our results demonstrate that intracellular proteins, released by injured neurons in the PNS, activate SC LRP1 in a manner that activates or sustains the SC Repair Program.

2 | MATERIALS AND METHODS

2.1 | Animals

Male Sprague Dawley rats (170–200 g; 8–12 weeks old) were purchased from Envigo (Indianapolis, USA). Male and female C57BL/6J mice (25 g; 8–12 weeks old) were purchased from Charles Rivers Laboratories (Wilmington, USA). Transgenic mice in which hemagglutinin (HA)-tagged ribosomal protein L22 is expressed under the control of *Cre recombinase* (Heiman et al., 2008; Sanz et al., 2009) were crossed with the B6N.FVB-Tg(Mpz-cre)26Mes/J that express Cre recombinase under the control of the P0 promoter in the C57BL/6J background (Feltri et al., 1999, 2002). These mice are called RiboTag-P0 mice. In this strain of P0-*Cre* mice, Cre recombinase is embedded in the complete endogenous mouse P0 regulatory domain and thus, there is a high level of specificity for SCs (Feltri et al., 1999; Feltri et al., 2002). Breeding this transgene into our mice will allow specificity to myelinating and non-myelinating SCs without contaminating RNA from other cells. Transgenic mice are genetically deficient in SC LRP1 (scLRP1$^{-/-}$) and littermate controls expressing SC LRP1 (scLRP1$^{+/+}$) in the C57BL/6 background are previously described (Orita et al., 2013; Poplawski et al., 2018). In scLRP1$^{+/+}$ mice, both genes encoding LRP1 are partially flanked by loxP sites, as in scLRP1$^{-/-}$ mice; however, scLRP1$^{+/+}$ mice are P0-Cre recombinase-

TABLE 1 Proteins and reagents used in the study (alphabetical order).

Protein/reagent	Catalog no.	Supplier
AZD0530 (Saracatinib)	11497	Cayman Chemical
Cell Line Nucleofector Kit V	VCA-1003	Lonza
Collagenase type I	17100017	ThermoFisher Scientific
DAPI	ab104139	Abcam
Fetal Bovine Serum (FBS)	10-082-147	Gibco
Forskolin	3828S	Cell signaling
iScript cDNA synthesis kit	1708891	Bio-Rad
Isoflurane	502017	IsoSol, VedCo
K252a	12754	Cell signaling
MK801	27213	Cayman Chemical
Neuregulin 1 (NRG1)	9875-NR-050	R&D System
Neurotrophin-3 (NT-3)	267-N3-005	R&D System
ON-TARGETplus Non-targeting Control Pool	D-001810-10-05	Horizon Discovery
ON-TARGETplus SMARTpool siRNA LRP1	L-101489-02-0005	Horizon Discovery
ON-TARGETplus SMARTpool siRNA Ntrk3	L-091405-02-0005	Horizon Discovery
Recombinant Human Decorin Protein	143-DE-100	R&D System
Recombinant Human PACSIN1/Syndapin-1	C834	Bon Opus Biosciences
Penicillin/Streptomycin (P/S)	P1476	Millipore Sigma
pFUSE-rIgG-Fc2	pfuse-rfc2	Invivogen
PP2	ab120308	Abcam
Protein A-Sepharose 4B	P9424-1ML	Scientific Laboratory Supplies
SuperSignal West Pico PLUS Chemiluminescent Substrate	PI34578	ThermoFisher Scientific
TaqMan Gene Expression Assay, rat ARID4B	Rn00670422_m1	ThermoFisher Scientific
TaqMan Gene Expression Assay, rat Egr1	Rn00561138_m1	ThermoFisher Scientific
TaqMan Gene Expression Assay, rat GAPDH	Rn99999916_s1	ThermoFisher Scientific
TaqMan Gene Expression Assay, rat Ntkr2	Rn01441749_m1	ThermoFisher Scientific
TaqMan Gene Expression Assay, rat Ntkr3	Rn00570389_m1	ThermoFisher Scientific
TaqMan Gene Expression Assay, rat Vcan	Rn01493755_m1	ThermoFisher Scientific

negative. Experiments comparing all transgenic mice were performed using 3–5 month-old female littermates. Breeding procedures and animal experiments were performed according to protocols approved by the Veterans Administration (VA) and conform to VA Guidelines for Animal Use. Rodents were housed using a 12 h:12 h light:dark cycle with ad libitum access to food and water.

2.2 | Proteins and reagents

Proteins and reagents used in the present study are listed in Tables 1 and 2.

2.3 | Sciatic nerve crush injury

Mice and rats were subjected to sciatic nerve crush injury or sham operation. Mice were anesthetized with 3% isoflurane and maintained with 2% isoflurane. Rats were anesthetized with 5% isoflurane (IsoSol, VedCo, Saint Joseph, USA) and maintained with 2.5% isoflurane. An incision was made along the long axis of the femur. The sciatic nerve was exposed at the mid-thigh level by separating the biceps femoris and the gluteus superficialis and then carefully cleared of surrounding connective tissue. In mice, the sciatic nerve was crushed twice for 15 s with flat forceps, and in rats, the sciatic nerve was crushed for 30 s with flat forceps (Azzouz et al., 1996; Poplawski et al., 2018). The site of the crush injury was marked with an epineural suture or ink at the muscle surface. The muscle and skin layers were closed using silk sutures. Nerves at the crush site and distal to the injury were collected 24 h after the crush injury.

2.4 | Isolation of nerve extracts for LC–MS/MS and validation studies

Sciatic nerves that are distal to crush injury sites were desheathed by removing the epineurium with stainless steel Moria forceps (Antony, France). The epineurium was removed and the endoneurium was subsequently digested with 1.0% (w/v) collagenase type I for 45 min at 37°C to prevent cell lysis. Nerve digests with intact cells were centrifuged at $1500 \times g$ for 10 min. Supernatants containing only extracellular proteins were collected and protein levels were determined by bicinchoninic acid (BCA) assay kit (Pierce) and were subsequently subjected to immunoblot analysis. Control nerves were extracted using a standard procedure that yields cellular proteins in RIPA buffer (nerve extract) after desheathing and also subjected to immunoblot analysis.

2.5 | Immunoblotting

Protein in tissue and cell extracts was determined by BCA assay. Protein extracts (10 or 20 μg/lane) were subjected to SDS-PAGE on

TABLE 2 Antibodies used in the study (alphabetical order).

Antibody	Host	Dilution	Catalog #	Supplier	Application	RRID
Alexa Fluor 488	Mouse	1:500	A-21202	ThermoFisher Scientific	IF	AB_141607
Alexa Fluor 488	Rabbit	1:500	A-11034	ThermoFisher Scientific	IF	AB_2576217
Alexa Fluor 594	Mouse	1:500	A-11032	ThermoFisher Scientific	IF	AB_2534091
Alexa Fluor 594	Rabbit	1:500	A-21442	ThermoFisher Scientific	IF	AB_2535860
ßIII Tubulin	Rabbit	1:1000	5666	Cell Signaling Technology	WB	AB_10691594
β Actin	Mouse	1:1000	3700	Cell Signaling Technology	WB	AB_2242334
p-C-Jun	Rabbit	1:1000	9261	Cell Signaling Technology	WB	AB_2130162
t-C-Jun	Rabbit	1:1000	9165	Cell Signaling Technology	WB	AB_2130165
p-ERK	Rabbit	1:1000	9101	Cell Signaling Technology	WB	AB_331646
t-ERK	Rabbit	1:1000	9102	Cell Signaling Technology	WB	AB_330744
GAPDH	Rabbit	1:1000	5174	Cell Signaling Technology	WB	AB_10622025
GST	Rabbit	1:1000	2622	Cell Signaling Technology	WB, IP	AB_331670
LRP1	Rabbit	1:1000	64,099	Cell Signaling Technology	WB	AB_2799654
MMP9	Mouse	1:1000	MA5-45511	ThermoFisher Scientific	WB, IP	AB_2931965
MP0	Rabbit	1:300	ab183868	Abcam	IHC, IF	AB_2895675
PACSIN1	Rabbit	1:1000	ab137390	Abcam	WB, IP	AB_2920903
PACSIN1	Rabbit	1:300	NBP1-87067	Novus Biologicals	IHC, IF	AB_11015143
S100 β	Rabbit	1:100	ab52642	Abcam	IF	AB_882426
p-TrkC	Rabbit	1:1000	3376	Cell Signaling Technology	WB	AB_2155283

Abbreviations: IF, Immunofluorescence; IHC, Immunohistochemistry; IP, Immunoprecipitation; WB, Western Blot.

8%–12% gradient gels and then, electrotransferred to nitrocellulose or PVDF membranes using a BioRad Trans-Blot Turbo Transfer System (Hercules, CA). Membranes were blocked with blotting grade blocker (5% nonfat dry milk) (#170-6404, Bio Rad, Irvine, USA) or bovine serum albumin (BSA) (#97061-420, VWR, Swedesboro, USA) in 10 mM Tris–HCl, 150 mM NaCl, pH 7.5, 0.1% Tween 20 (TBS-T) for 1 h at room temperature. Primary antibodies (Table 1) diluted in 5% BSA/TBS-T or MILK/TBS-T were incubated with the membranes overnight at 4°C. Membranes were washed with TBS-T and incubated with horseradish peroxidase (HRP)-conjugated secondary anti-mouse IgG (#7076, Cell Signaling, Danvers, USA) or anti-rabbit IgG (#7074, Cell signaling, Danvers, USA) in TBS-T with nonfat dry milk for 1 h at 22°C followed by enhanced chemiluminescence (ECL, ThermoFisher Scientific, Waltham, USA). Blots were imaged using a BioRad Chemi-Doc Imaging System (Hercules, CA).

2.6 | LRP1 ligand capture using LRP1 CCR2 and CCR4-fusion proteins

Ligand-binding to LRP1 occurs mainly via the LRP1 CCR2 and CCR4 motifs (Strickland et al., 2002). We expressed human CCR2 and CCR4 as Fc fusion proteins, as previously described (Fernandez-Castaneda et al., 2013; Stiles et al., 2013). Collagenase extracts (250–300 μg) were incubated with CCR2 or free Fc (30 μg), as a control, for 12 h at 4°C. Equivalent amounts of CCR2, CCR4, or free Fc also were incubated with the known LRP1 ligand, MMP-9-PEX, expressed as

GST fusion proteins and purified as previously described (Mantuano et al., 2008), or with sciatic nerve extracts containing possible LRP1 ligands. The Fc fusion proteins were then captured with Protein A-Sepharose, washed extensively, and eluted for LC–MS/MS (Fernandez-Castaneda et al., 2013; Gaultier et al., 2010).

2.7 | LC–MS/MS and analysis by mass spectrometry interaction statistics

CCR2-captured ligands were subjected to trypsin digestion in the presence of ProteaseMax surfactant for LC–MS/MS. Tryptic peptides were passed through C18 spin tips, eluted in 80% acetonitrile/0.1% formic acid, vacuum-dried, equilibrated in 1% acetonitrile/0.1% formic acid, packed into 70 μm C18 infused capillaries, and eluted in a positive-ion nanospray with a 1%–90% acetonitrile gradient using an Agilent 1200 series liquid chromatography injection system. Peptides were detected with an LTQ OrbiTrap XL MS using Xcalibur 2.1. For the assignment, raw files were searched against species-specific proteomes, using Proteome Discoverer Software 2.0 with SEQUEST HT and MS Amanda search engines. Our search parameters identified fixed modifications, including cysteine carbamidomethylation, variable methionine oxidation, lysine carbamylation, and N-terminal acetylation and oxidation. The maximum number of missed cleavages permitted was two. Mass tolerance for precursor ions was set to 50 ppm and for fragment ions, 0.6 Da. Peptides with an Xcorr threshold ≤1% were subjected to validation through the MS Amanda search engine.

A strict peptide false-positive rate of 5% was used to accept proteins based on spectral match. Each distinct sample was analyzed in technical triplicates. Proteins identified in the extracellular spaces of rat or mouse crush-injured sciatic nerves are reported. Mass spectrometry interaction STatistics (MiST) scores were calculated, based on the abundance of the protein captured, reproducibility of capture, and specificity relative to the control bait (Free Fc; Verschueren et al., 2015). CCR2/CCR4-binding interactions that generated MiST scores higher than 0.84 are reported.

2.8 | Immunohistochemistry of DRGs and sciatic nerves

Naïve mice and mice that had been subjected to crush injury were initially anesthetized with 3% isoflurane (IsoSol, VedCo, Saint Joseph, USA) in 1.5 L/min oxygen and maintained under 2% isoflurane. Dorsal root ganglia (DRG) were collected by making a spinal column transection at the final pair of ribs (into caudal and rostral segments). L3, L4, and L5 DRGs were then collected. DRGs and sciatic nerves were embedded in paraffin, and IHC studies were performed as previously described (Wang et al., 2022). Briefly, 1–5 μm thick DRG or nerve tissue sections were immunostained for PACSIN1. Slides were immunostained using a Ventana Discovery Ultra (Ventana Medical Systems, Oro, USA). Antigen retrieval was performed using CC1 (tris-based; pH 8.5) for 40 mins at 95°C. The primary antibody targeting PACSIN1 was incubated with the slides for 32 min at 37°C. The secondary antibody, OmniMap anti-HRP (#760-4311, Ventana Medical Systems, Oro, USA), was incubated on the sections for 12 min at 37°C. Antibodies were visualized using diaminobenzidine as a chromogen followed by hematoxylin as a counterstain. Slides were rinsed, dehydrated through alcohol and xylene, and coverslipped. Light microscopy was performed using a Leica DFC420 microscope with Leica Imaging Software 2.8.1 (Leica Biosystems, Vista, USA).

In some cases, dual chromagenic or immunofluorescence (IF) staining for PACSIN1 was performed on DRG or transverse sections of sciatic nerves. Sciatic nerves were collected as described above. We utilized the anti-PACSIN1 antibody (Novus, Centennial, CO) and the OmniMap detection system HRP-coupled goat anti-rabbit (Ventana Medical Systems, Tucson, USA) followed by either chromogenic labeling with Ventana Purple kit according to the manufacturer's instructions or with TSA-Alexa 488. For both dual IHC and dual IF, endogenous antibodies were fully denatured, inactivated, and removed from the tissue by treatment in CC2 citrate-based, pH 6.5 (Ventana Medical Systems, Tucson, USA) for 20 min at 100°C. Subsequently, the primary antibody was applied and detected by the OmniMap system (Ventana Medical Systems, Tucson, USA). Chromogenic labeling for P0-expressing cells used the Ventana Green kit followed by hematoxylin counterstain whereas for dual IF (P0 or HA-tag) the OmniMap system was followed by incubation with Alexa-594 (red). Immunohistochemistry slides were rinsed, dehydrated in alcohols, cleared in xylene, and coverslipped while IF slides were rinsed and coverslipped with Vectashield containing DAPI (Vectorlabs).

Immunofluorescence was imaged using an Axio imager Z2 with calibri7 LED equipped with Plan-Apochromat 20x/0.8 M27 objective and Plan-Apochromat 63×/1.40 Oil DIC M27 objective. The cells were stimulated with the 358 nm (blue channel), 385 nm (green channel), and 475 nm (red channel). The light-emitting diode intensity was set at 5% (blue channel) and 10% (green and red channels). 3008×4096 pixels images were acquired and analyzed with ZEN 3.6 (ZEN pro) software.

2.9 | Rat primary SC cultures

Primary rat SC cultures (SCs) were isolated from postnatal (day 1) rat pups and maintained as described previously (Campana et al., 2006; Sadri et al., 2022). Schwann cells were cultured in complete medium consisting of Dulbecco's Modified Eagle Medium (DMEM) (#11885, Gibco, Billings, USA), supplemented with 10% heat-inactivated FBS (#10–082-147, Gibco, Billings, USA), 100 U/mL penicillin, 100 μg/mL streptomycin, 21 μg/mL bovine pituitary extract (#P1476, Millipore Sigma, St. Louis, USA), and 4 μM forskolin (#3828S, Cell signaling, Danvers, USA) at 37°C in humidified atmosphere with 5% CO_2. To confirm the purity of the primary cultures, isolated SCs were immunostained with anti-S100β and Dapi. Schwann cells were determined to be greater than 90% pure. Schwann cells used for all studies were passaged no more than six times.

2.10 | Gene silencing with transient siRNAs

Rat-specific ON-TARGETplus SMARTpool siRNA, stargeting *Lrp1* or *Ntrk3* and pooled NTC siRNA were from Horizon Discovery. Schwann cells were transfected with siRNA by electroporation using the Cell Line Nucleofector Kit V (#VCA-1003, Lonza, Houston, USA), following the manufacturer's instructions. Briefly, cell suspensions were combined with *Lrp1*-specific (200 nM), *Ntrk2*-specific (100 nM), *and Ntrk3*-specific (100 nM) or NTC siRNA (200 or 100 nM, respectively), and electroporated with a SCs-specific program in a Nucleofector 2b device (Lonza, Houston, USA). The efficiency of gene silencing was validated 48 h after transfection by reverse transcriptase polymerase chain reaction (RT-qPCR) and immunoblotting (Figures S1 and S3). Experiments were performed 48 h after transfection.

2.11 | Cell signaling in vitro and in vivo

Schwann cells (2.5×10^5 cells per well) were seeded in PDL-coated 6-well plates at a density of and cultured in the complete medium until ~80% confluent. Cells were serum-starved for 1 h and treated with various proteins, including PACSIN1 (#C834, Bon Opus Biosciences, Millburn, NJ, USA); Decorin, (#143-DE-100, R&D System, Minneapolis, USA), alpha-2-macroglobulin (α2M), Neurotrophin-3 (NT-3) (#267-N3-005, R&D System, Minneapolis, USA) or Neuregulin-1 (NRG1) (#9875-NR-050, R&D System, Minneapolis, USA). In some

cases, SCs were pretreated with MK801 (1 μM) (#27213, Cayman Chemical, Ann Arbor, USA), PP2 (1 μM) (#ab120308, Abcam, Cambridge, USA), AZD0530 (20 nM) or K252a (100 nM) (#12754, Cell signaling, Danvers, USA) prior to the addition of protein. Cells were lysed in RIPA buffer and protein extracts were immunoblotted as described above.

To study cell-signaling in vivo, scLRP1$^{-/-}$ and scLRP1$^{+/+}$ mice were subjected to crush injury as described above. Twenty-four hours following the crush injury and under isofluorane anesthesia, sciatic nerves were exposed and PACSIN1 (1 μM in 2 μL) or vehicle (PBS) was injected intraneurally, distal to the crush injury in the sciatic nerve, using a 5 μL Hamilton syringe with a 32-gauge needle. After 15 min, nerve tissue was collected and lysed in RIPA buffer for immunoblot analyses.

2.12 | SC migration assay

Migration of primary rat SCs was studied using 6.5 mm Transwell chambers with 8 μm pores (#3422, Corning Costar, Cambridge, USA) as described previously (Mantuano et al., 2008; Nguyen et al., 1999). The bottom surface of each membrane was coated with 10 μg/mL fibronectin for 2 h at 37°C. We selected fibronectin as the substratum because, after peripheral nerve injury, fibronectin expression is induced to provide a provisional matrix for nerve regeneration (Akassoglou et al., 2002). Schwann cells (1.0 × 10^4 cells per top chamber) were seeded in Sato medium supplemented with 1 mg/mL BSA (Bottenstein & Sato, 1980) and were subsequently treated with vehicle, NRG-1 (0.2 nM), or PACSIN1 (10 nM or 25 nM) for 10 min at 37°C. Reagents were added only to the top chambers of the Transwells. The bottom chamber contained 10% FBS. Cells were allowed to migrate at 37°C in 5% CO$_2$. After 3 h, the upper surface of each membrane was cleaned with a cotton swab. The membranes were then stained with Diff-Quik (#564-850-02, Dade-Behring, Deerfield, USA). The number of cells migrating to the bottom surface of each membrane was counted. Each condition was studied in triplicate. Three fields were examined per filter.

2.13 | Apoptosis, cell death, and viability studies

To measure apoptosis, we utilized the terminal deoxynucleotidyl transferase biotin-dUTP nick end labeling (TUNEL) kit (#ab66108, Abcam, Cambridge, USA), which measures DNA fragmentation. Schwann cells (1.0 × 10^6 cells) were seeded in a T25 flask. After the cells were attached, cells were gently washed and cultured in DMEM-low glucose medium without serum for 90 min. Subsequently, the medium was replaced with DMEM containing 0.5% FBS, in the presence or absence of PACSIN1 (50 nM) for 6 h. Some cultures were pre-treated with PP2 (1 μM) or K252a (100 nM) during the 90 min starvation. TUNEL staining was performed following the manufacturer's protocol. Propidium iodide/RNase in the kit was used to stain cell nuclei. Images of TUNEL-positive SCs were collected with an

Olympus IX73 microscope with an attached ORCA-FLASH camera and Infinity Analyze and Capture Software. Quantitative fluorescence imaging was acquired with equivalent microscope settings.

The Cell Death ELISA™ (#11774425001, Roche Applied Science, Indianapolis, USA) kit measures cytoplasmic histone-associated DNA fragments (mono and oligosomes). Schwann cells (1.0 × 10^4 cells per well) were seeded in 96-well plates. After the cells were attached, cells were gently washed and cultured in DMEM medium with no serum for 90 min. Subsequently, the medium was replaced with DMEM containing 0.5% FBS, in the presence or absence of PACSIN1 (50 nM) for 18 h. Some cultures were pre-treated with PP2 (1 μM) or K252a (100 nM) for 90 min. SCs cultured in 10% FBS-containing media served as normalizing controls. SC death was detected by colorimetric analyses (402 nm). ELISA plates were read on Molecular Devices SpectraMax 384 Plus (Thermo Fischer).

To measure SC viability, we performed Trypan Blue staining studies. Schwann cells (2.0 × 10^5 cells per well) were seeded in 6 well plates. After the cells were attached, cells were gently washed and cultured in DMEM medium with no serum for 90 min. Subsequently, the medium was replaced with DMEM containing 0.5% FBS, in the presence or absence of PACSIN1 (50 nM), for 6 h. Some cultures were pre-treated with PP2 (1 μM) or K252a (100 nM) for 90 min. SCs cultured in 10% FBS-containing media served as controls. Cells were loaded onto a hemocytometer for counting both clear and blue cytoplasm-colored cells on an Olympus CXK41 microscope.

2.14 | Bulk RNA-Seq and bioinformatic analysis

Schwann cells (2.0 × 10^5 cells per well) were seeded in 6-well plates and allowed to attach in a complete medium overnight. Cells were gently washed and cultured in DMEM without serum for 60 min. Subsequently, the medium was replaced with DMEM containing 0.5% FBS, in the presence or absence of PACSIN1 (50 nM) for 5 h. Total RNA was extracted from the SCs in Trizol® and purified using the Nucleospin RNA kit (Macherey-Nagel, Düren, Germany). RNA samples were analyzed by the Institute of Genomic Medicine, University of California, San Diego. RNA was assessed for quality using an Agilent Tapestation 4200. RNA Sequencing libraries generated from samples with an RNA Integrity number (RIN) greater than 8.0 were prepared using the TruSeq stranded mRNA sample prep kit with TruSeq Unique Dual Indexes (Illumina, San Diego, USA). Profiling was conducted with an Illumina NovaSeq 6000 Illumina. Samples were demultiplexed using bcl2fastq v2.20 Conversion Software (Illumina, San Diego, CA). Quality control of the raw fastq files was performed using the software tool FastQC (Andrews, 2010) v0.11.8. Sequencing reads were trimmed with Trimmomatic (Bolger et al., 2014) v0.38 and aligned to the rat genome, (mRatBN7.2: genomic reference consortium) using the STAR aligner (Dobin et al., 2013) v2.5.1a. Read quantification was performed with RSEM (Li & Dewey, 2011) v1.3.0 and the Ensembl release 107 annotation. The R BioConductor packages edgeR (Robinson et al., 2010) and limma (Ritchie et al., 2015) were used to implement the limma-voom (Law et al., 2014) method for differential

expression analysis. In brief, low expressing genes, those not having counts per million (cpm) ≥ 1 in at least 3 of the samples, were filtered out, and then trimmed mean of M-values (TMM) (Robinson et al., 2010) normalization was applied. The experimental design was modeled upon condition and batch ($\sim 0 +$ condition + batch). The voom method was employed to model the mean–variance relationship in the log-cpm values weighted for inter-subject correlations in repeated measures of patients, after which lmFit was used to fit per-gene linear models, and empirical Bayes moderation was applied with the eBayes function. Significance was defined by using an adjusted p-value cut-off of 0.4 after multiple testing corrections (Benjamini & Hochberg, 1995) using a moderated t-statistic in limma and a minimum absolute log-fold-change threshold of 0.

2.15 | RT-qPCR

RNA was reverse-transcribed using the iScript cDNA synthesis kit (Bio-Rad, Hercules, USA). RT-qPCR was performed using TaqMan™ gene expression products and the CFX Connect Real-Time system (Bio-Rad, Hercules, USA). The relative change in gene expression was calculated using the $2^{\Delta\Delta Ct}$ method. GAPDH mRNA was measured as a standard. The primer-probe sets used included: *ARID4B* (#Rn00670422_m1), *Egr1* (#Rn00561138_m1), *VCAN* (#Rn01493755_m1), *Ntrk2* (#Rn01441749_m1), and *Ntrk3* (Rn000570389_m1), and normalized to GAPDH (#Rn99999916_s1). All probes were purchased from Thermo-Fisher Scientific, Waltham, USA (see Table 1). The relative change in mRNA expression was calculated using the $2^{\Delta\Delta CT}$ method with GAPDH mRNA as an internal normalizer. All results are presented as the fold-change in mRNA expression relative to controls.

2.16 | Statistics

Statistical analysis was performed using GraphPad Prism 5.0 (GraphPad Software). Results are presented as the mean ± SEM. Cell-signaling, cell survival assays, and migration assay data were analyzed by one-way analysis of variance (ANOVA) followed by a Tukey's or Dunn's post hoc test (*p < .05; **p < .01; ***p < .001, ****p < .001) or Kruswalis analysis (for nonparametric data) with a Mann–Whitney U post hoc test. A Student's t-test was used when only two means were compared.

3 | RESULTS

3.1 | Identification of LRP1 ligands in the extracellular spaces of sciatic nerves

We sought to identify novel LRP1 ligands that are present in the extracellular spaces of the sciatic nerve after nerve injury. To accomplish this goal, we extracted and digested nerve tissue with collagenase 1. This was important because we wanted to identify proteins
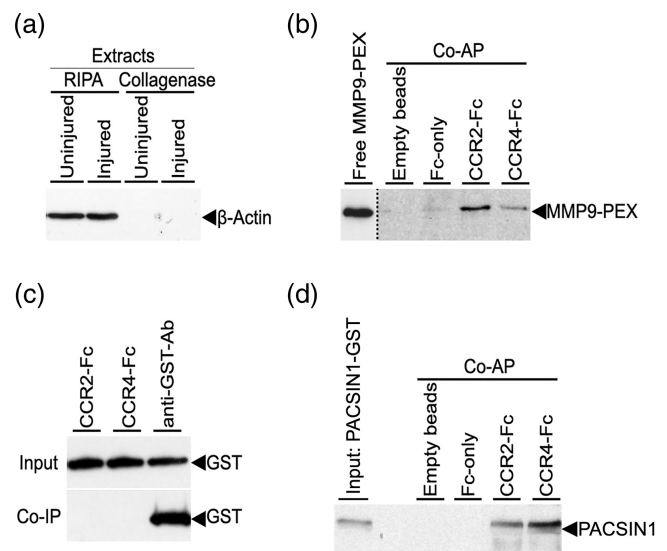

FIGURE 1 Isolation of proteins in the extracellular spaces of sciatic nerves and validation of LRP1 binding domain fusion proteins. (a) Uninjured nerves and crush-injured nerves (after 24 h) treated with collagenase 1 solution or RIPA lysis buffer were loaded into each lane (10 μg). Protein lysates were subjected to immunoblot analysis to detect cellular β-Actin. (b) Fc-fusion proteins of the CCR2 and CCR4 LRP1 binding domains, Fc-only and protein A-Sepharose beads were incubated (12 h at 4°C) with a known LRP1 ligand, MMP-9-PEX, that contains a glutathione-S-transferase (GST) fusion protein tag. Affinity precipitates (co-AP) were subjected to immunoblot analyses to detect GST. (c) CCR2 and CCR4 were incubated with recombinant GST, which failed to bind CCR2 or CCR4. In contrast, an antibody to GST co-immunoprecipitated GST. (d) Purified recombinant human PACSIN1, expressed as a GST fusion protein, was incubated with Fc-CCR2 and Fc-CCR4, or free Fc coupled to protein agarose beads. Affinity precipitates (co-AP) were subjected to immunoblot analyses to detect GST-PACSIN1. Blots represent $N = 3$ replicates.

released during nerve injury and not during our extraction procedure. To confirm that the collagenase extracts contained only extracellular proteins from the sciatic nerve, equal amounts of protein from RIPA and collagenase extracts of uninjured nerve were subjected to immunoblot analysis for cellular β-actin. Sciatic nerves that had been subjected to crush injury 24 h prior were also examined. Figure 1a shows that actin was detected only in the RIPA extracts (cellular) and not in the collagenase extracts (non-cellular) post-injury.

To identify LRP1 ligands in the sciatic nerve collagenase 1 extracts, we expressed the ligand-binding motifs in LRP1, human CCR2 and CCR4, as Fc-fusion proteins as previously described (Fernandez-Castaneda et al., 2013; Stiles et al., 2013). CCR2, which includes amino acids 804-1185 of mature LRP1 and CCR4, which includes amino acids 3331-3778, have ligand-binding specificities that are highly overlapping (Mikhailenko et al., 2001). LRP1 is highly conserved, showing greater than 97% sequence identity between human and rat CCR2 and CCR4 (BLAST). To validate our methodology, equivalent amounts of CCR2, CCR4, or free Fc, as a control, were incubated with the known LRP1 ligand, MMP-9-PEX. Fc fusion proteins and associated proteins were isolated using Protein A-Sepharose beads. As shown in Figure 1b,

TABLE 3 LRP1 ligands captured from rat injured sciatic nerve.

MiST score	Entry	Protein name	
0.99354	P08649	Complement C4	
0.9906	P68370	Tubulin alpha-1A chain	
0.98884	P16638	ATP-citrate synthase	
0.98884	Q4V7E8	Leucine-rich repeat flightless-interacting protein 2	
0.98884	P19527	Neurofilament light polypeptide (NF-L)	
0.98605	Q63041	Alpha-1-macroglobulin (Alpha-1-M)	Known LRP1 ligands
0.98554	Q01129	Decorin	
0.98463	P12839	Neurofilament medium polypeptide (NF-M)	
0.98392	O35763	Moesin (membrane-organizing extension spike protein)	
0.98241	O55148	Growth arrest-specific protein 7 (GAS-7)	
0.87977	Q9Z0W5	Protein kinase C and casein kinase substrate in neurons protein 1	
0.87961	P21707	Synaptotagmin-1 (Synaptotagmin I) (Syt I) (p65)	
0.87809	P31977	Ezrin (Cytovillin) (Villin-2) (p81)	
0.87539	Q9QUR2	Dynactin subunit 4 (Dynactin subunit p62)	
0.87539	Q66H98	Serum deprivation-response protein (Cavin-2)	
0.87332	Q5XI32	F-Actin-capping protein subunit beta (CapZ beta)	
0.8584	P62944	AP-2 complex subunit beta	
0.85679	Q64119	Myosin light polypeptide	
0.84537	P05942	Protein S100-A4	

Note: The blue shade identifies previously known LRP1 ligands and the yellow shade identifies the neuronal protein captured in the nerve, and analyzed in this study.

MMP-9-PEX bound to CCR2 and CCR4, but not to Fc. Empty protein A-Sepharose A beads also failed to bind MMP9-PEX. Because MMP-9-PEX is expressed as a glutathione-S-transferase (GST) fusion protein, as a further control, we also incubated recombinant GST with CCR2 and CCR4. No binding was observed (Figure 1c); however, when we incubated GST with an antibody that recognizes GST, we recovered GST. We concluded that the Fc-fusion proteins, CCR2 and CCR4, are functional in LRP1 ligand binding and may be used to identify novel LRP1 ligands.

Next, CCR2, CCR4, and Fc were incubated with injured sciatic nerve collagenase extracts. Associated proteins were recovered by protein A-Sepharose pulldown and trypsin-digested. The resulting peptides were identified by LC–MS/MS. To judge the reliability of identified CCR2 or CCR4-binding interactions, we calculated MiST scores, which are based on the abundance of the protein captured, reproducibility of capture, and specificity relative to the control bait (Free Fc) (Verschueren et al., 2015). Table 3 reports CCR2/CCR4-binding interactions that generated MiST scores higher than 0.84, which is below the theoretically maximal MiST score of 1.0 but above a typically chosen threshold of 0.75 (Verschueren et al., 2015). Two known LRP1 ligands, α_1M and decorin (Gonias et al., 1983; Mikhailenko et al., 2001; Neels et al., 1999), were identified in the extracellular spaces of sciatic nerves subjected to crush injury. Among the 20 CCR2-binding proteins with the highest MiST scores, many were intracellular proteins. Intracellular proteins identified as CCR2 ligands selectively expressed in the nervous system, as reported in The Protein Atlas (Moreno et al., 2022), included neurofilament-light

chain, a nerve injury biomarker secreted into cerebrospinal cord fluid and serum (Hermesdorf et al., 2023), neurofilament medium peptide, growth-arrest specific protein 7, PACSIN1, and synaptotagmin 1. PACSIN1 was previously identified as an LRP1 ligand in myelin vesicles harvested from rodent brains using CCR-2/4-binding and LC–MS/MS (Fernandez-Castaneda et al., 2013). Thus, we chose to validate PACSIN1 as an LRP1 ligand and determine its efficacy PACSIN1 in triggering LRP1-dependent cell-signaling.

Purified recombinant human PACSIN1, which was expressed as a GST-fusion protein, was incubated with Fc-CCR2, Fc-CCR4, and free Fc, as a control. Figure 1d shows that PACSIN1 is bound to CCR2 and CCR4, as determined by immunoblot analysis of Protein A-Sepharose affinity precipitates. PACSIN1 failed to bind to free Fc or empty beads. These results demonstrate that PACSIN1 is an LRP1 ligand.

3.2 | PACSIN1 is localized to primary sensory neurons

To identify cell types in the DRG that express PACSIN1, we performed IHC studies with a PACSIN1-specific antibody (Novus, Centennial, CO) that does not cross to PACSIN2 or PACSIN3. PACSIN1 was expressed in both small and large-diameter neuronal cell bodies and axons of uninjured DRGs (Figure 2a). DRGs collected 1-day post-crush injury also showed PACSIN1 immunoreactivity specific to neurons (Figure 2a, middle and right panels). To identify the cell source of PACSIN1, we performed chromogenic dual immunostaining for PACSIN1 and the SC
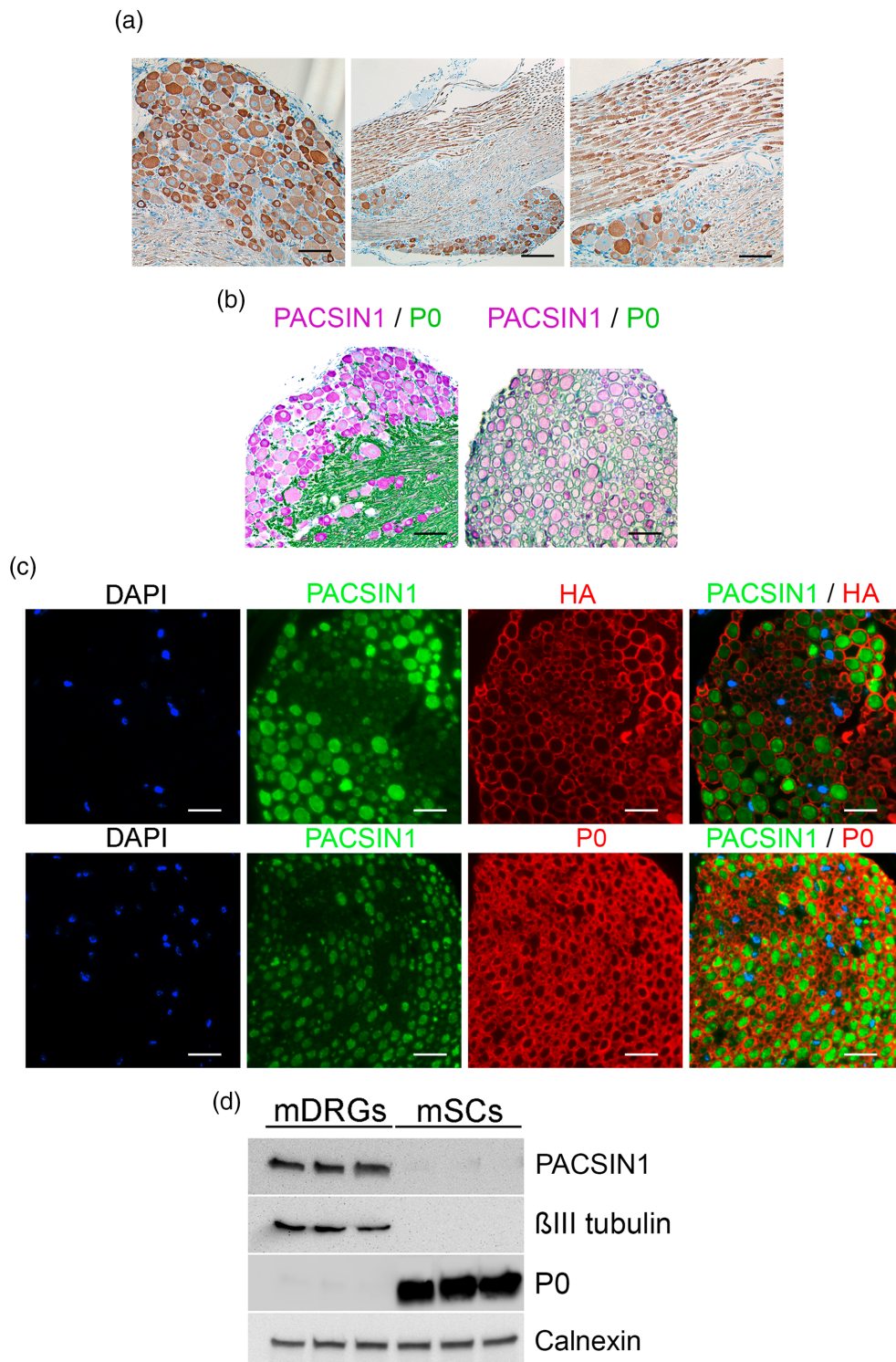
FIGURE 2 PACSIN1 is specifically localized to DRG neurons. (a) Paraffin-embedded uninjured (left panel) and 24 h post-injured (middle-10× and right-40× panel) mouse DRG sections were subjected to immunohistochemistry using an antibody that specifically recognizes PACSIN1. PACSIN1 immunoreactivity is shown in brown and the counterstain hematoxylin is in blue. Note that PACSIN1 was specifically expressed in small and large-diameter neuronal cell bodies and axons in naïve and injured nerves. Scale bar: 70 μm (left and right panel); Scale bar 300 μm (middle panel). Images represent $n = 4$ mice/group. (b) Paraffin-embedded uninjured mouse DRG sections (left) and transverse sciatic nerves (right) were subjected to chromogenic dual immunostaining for PACSIN1 (purple) and the compact myelin protein zero (green). Scale bar: DRG, 100 μM (left) and sciatic nerve, 50 μm. Images represent $N = 3–4$ replicates. (c) Transverse sciatic nerves from uninjured Ribo-Tag-P0-Cre mice were utilized for dual label immunofluorescence staining for HA (red) and PACSIN1 (green; Upper panel) or P0 (red) and PACSIN1 (green; lower panel). PACSIN1 was clearly identified in small and large myelinated fibers while HA was identified in SC cytoplasm, and P0 was identified in SC myelin, as anticipated. No co-localization was observed. Scale bar: 50 μM. Images represent $n = 3$ mice nerves. (d) Protein extracts from three individual mouse DRGs and three independent cell extracts from mouse primary cultured SCs (mSCs) were subjected to immunoblot analysis to detect PACSIN1, βIII-tubulin, and P0 to confirm the cellular source of the samples. Calnexin served as a loading control.

biomarker for compact myelin protein, P0, in uninjured mouse DRGs and sciatic nerves. PACSIN1 (purple) was localized to neuronal cell bodies and axons and did not overlap with P0 (green) in DRGs (Figure 2b, left panel) or in sciatic nerves (Figure 2b, right panel).

To further confirm our initial IHC findings, we utilized Ribo-Tag-P0-Cre mice that upon Cre recombination express an HA tag only in myelinating and nonmyelinating Schwann cells. We performed dual-label immunofluorescence for HA and PACSIN1 in transverse sciatic nerve sections. PACSIN1 was clearly identified in small and large myelinated fibers and revealed a mosaic pattern of fluorescence intensity in the fibers, consistent with its expression profile in neuronal cell bodies. HA was identified in the SC cytoplasm, specifically in the inner glial loops and crescents surrounding the axons, as anticipated. There was no co-localization of PACSIN1 with HA (Figure 2c; upper panels).

Next, we performed dual-label immunofluorescence for P0 and PACSIN1 in sciatic nerves. Like our initial results with the chromogenic dual immunostaining (Figure 2b, right panel), co-localization of PACSIN1 with P0 was not observed (Figure 2c; lower panels).

Finally, we performed immunoblot studies of PACSIN1 in three individual mouse DRGs and three independent cellular extracts from primary cultured mouse SCs (mSCs). PACSIN1 was clearly identified with DRGs, but not mSCs (Figure 2d). A very faint higher molecular weight band was observed in mSCs, which is likely PACSIN2. PACSIN2 is abundantly expressed in glia (Thornhill et al., 2007) and the PACSIN1 antibody (Abcam, Cambridge, UK) used for immunoblotting shows some cross-reactivity to PACSIN2. BIII-tubulin was only identified in mouse DRGs whereas P0 was only identified in mSCs, as anticipated. Calnexin served as a loading control. Collectively, these
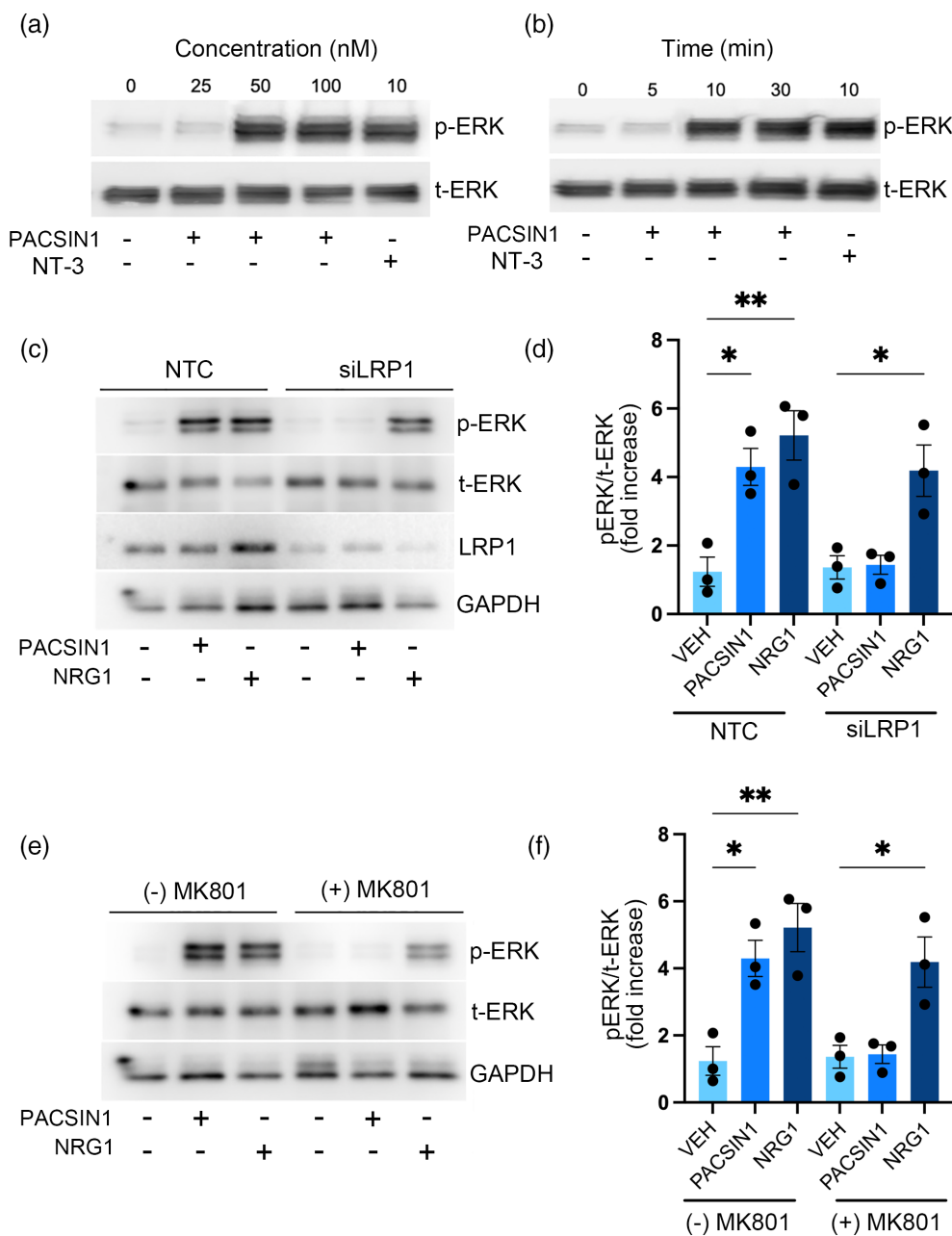

FIGURE 3 PACSIN1 activates LRP1-dependent phosphorylation of ERK1/2 in SCs. (a) Primary rat SCs (SCs) were treated with PACSIN1 (0–100 nM) or NT-3 (10 nM) for 10 min. (b) SCs were treated with PACSIN1 (50 nM) for 0–30 min. NT-3 (10 nM at 10 min) served as a control. For each experiment, cell extracts were subjected to immunoblot analysis to detect phospho-ERK1/2 and total ERK1/2. (c) SCs transiently electroporated with non-targeting control (NTC) or siRNA targeting LRP1 (si*LRp1*) were treated with PACSIN1 (50 nM) or NRG1 (2 nM) for 10 min. Cell extracts were subjected to immunoblot analysis to detect phospho-ERK1/2 and total ERK1/2. (d) Immunoblots were analyzed by densitometry. The ratios of p-ERK1/2 to t-ERK were calculated for each treatment group. (e) SCs were pre-treated for 30 min with MK801 (1 μM), and subsequently stimulated with PACSIN1 (50 nM) or NRG1 (2 nM). Cell extracts were subjected to immunoblot analysis to detect phospho-ERK1/2 and total ERK1/2. (f) Immunoblots were analyzed by densitometry. The ratio of p-ERK1/2 to t-ERK was calculated for each treatment group. Data are expressed as mean ± SEM of three independent studies and analyzed by one-way ANOVA and Tukey's post hoc test; (*$p < .05$ and **$p < .01$, compared to vehicle controls).

findings are consistent with studies of PACSIN1 expression patterns in the CNS, demonstrating that PACSIN1 is predominantly expressed in neurons (Grimm-Günter et al., 2008) and not glia.

3.3 | PACSIN1 activates LRP1-dependent cell-signaling in SCs

To evaluate the ability of PACSIN1 to activate cell signaling, we initially stimulated rat primary cultured SCs with different concentrations of human PACSIN1 (0–100 nM). PACSIN1 is highly conserved, showing greater than 95% sequence identity between human and rat (BLAST). PACSIN1 induced ERK1/2 activation at 50 nM and above after 10 min, but not at 25 nM (Figure 3a). Activation of ERK1/2 was similar in magnitude to that observed with NT-3 (10 nM).

Next, PACSIN1 (50 nM) was added to the cultures at different times (5, 10, and 30 min). ERK1/2 activation by PACSIN1 was observed within 10 min and sustained for 30 min (Figure 3b). When *Lrp1* gene expression was silenced with siRNA, as previously described (Mantuano et al., 2008), the LRP1 85-kDa β-chain was significantly decreased (>85%), as determined by immunoblot and densitometric analyses (Figure 1s; $p < .0001$). In LRP1-deficient SCs, PACSIN1 failed to induce ERK1/2 phosphorylation, however, the response to NRG1 remained unchanged (Figure 3c). Densitometric analyses of three independent studies demonstrated a greater than 4-fold increase in phospho-ERK1/2 ($p < .05$) in response to PACSIN1 that was blocked when *Lrp1* was silenced (Figure 3d).

LRP1 utilizes co-receptors to activate cell signaling (Mantuano et al., 2015; Mantuano et al., 2022; Rohrbach et al., 2021). In SCs, NMDA-R is a co-receptor for several LRP1 ligands, including tissue-type plasminogen activator (tPA) and MMP-9-PEX. We therefore tested whether the NMDA-R channel inhibitor, MK801, affects cell signaling in response to PACSIN1. Schwann cells were pre-treated with 1 μM MK801 for 30 min, and subsequently stimulated with PACSIN1 or NRG1. ERK1/2 phosphorylation in response to PACSIN1 was blocked by MK801 (Figure 3e). Densitometric analyses of three independent studies demonstrated a greater than 3.5-fold increase in phospho-ERK1/2 ($p < .0001$) in response to PACSIN1 that was blocked in the presence of MK801 (Figure 3f).

3.4 | PACSIN1 activates c-Jun, a key transcription factor in the SC repair program

We hypothesized that PACSIN1 is released from damaged axons into the extracellular spaces to activate SC LRP1 and repair signaling after peripheral nerve injury. Initially, we compared PACSIN1 signaling in SCs to other SC mitogens (NRG1, NT-3) and known LRP1 ligands identified in the extracellular space (decorin) that are capable of cell signaling (Figure 4s). PACSIN1 activated c-Jun. Next, we tested whether PACSIN1 at various concentrations (0–100 nM) activates c-Jun in primary cultured SCs. As shown in Figure 4a, PACSIN1 at 50 and 100 nM induced c-Jun phosphorylation. NT-3 (10 nM), a positive control, also activated c-Jun. Time-course studies revealed that PACSIN1 activated c-Jun within 10 min;

FIGURE 4 Activation of SC repair signaling is facilitated by PACSIN1 in vitro. (a) Primary rat SCs (SCs) were treated with PACSIN1 (0–100 nM) or NT-3 (10 nM) for 10 min. (b) SCs were treated with PACSIN1 (50 nM) for 0–30 min. NT-3 (10 nM) served as a control. (c) SCs transiently electroporated with non-targeting control (NTC) or siRNA targeting LRP1 (*siLrp1*) were treated with PACSIN1 (50 nM) or NRG1 (2 nM) for 10 min. For each experiment, cell extracts were subjected to immunoblot analysis to detect phospho-c-Jun and total c-Jun. (d) Immunoblots were analyzed by densitometry. The ratio of phospho-c-Jun to total-c-Jun was calculated for each treatment group. Data are expressed as mean ± SEM of three independent studies and analyzed by one-way ANOVA and Tukey's post hoc test (*$p < .05$ compared to vehicle controls).
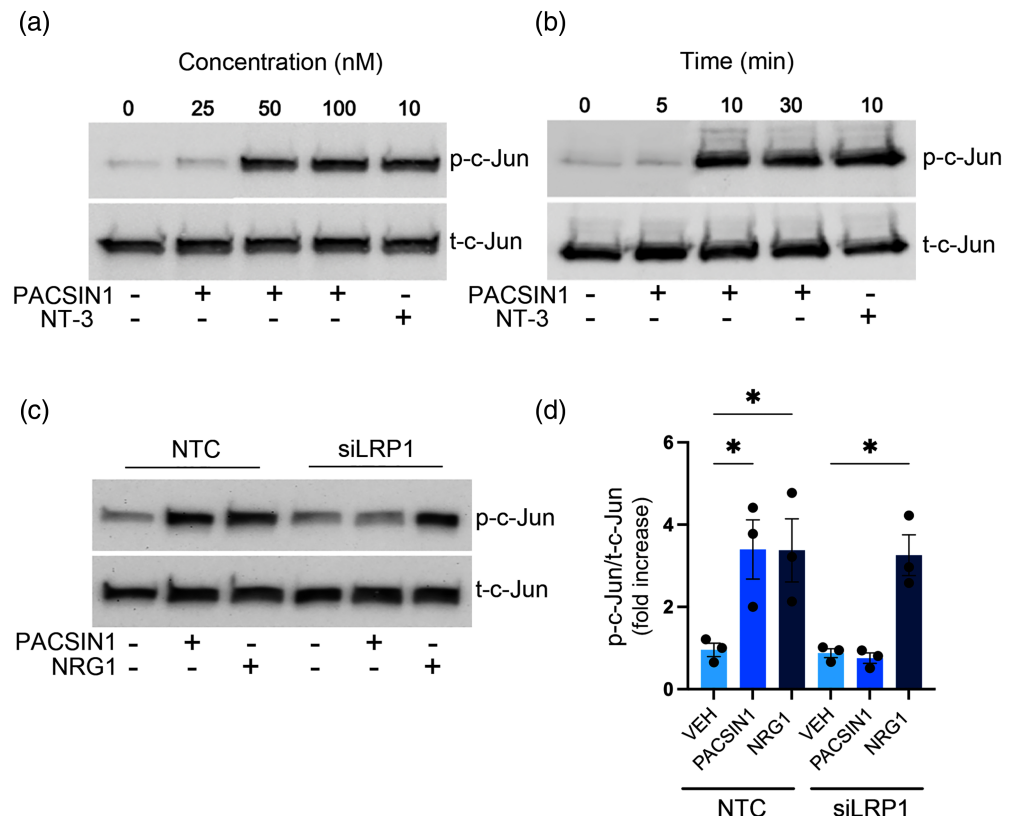
activation was sustained for 30 min (Figure 4b). When *Lrp1* gene expression was silenced in SCs with siRNA, activation of c-Jun by PACSIN1 was inhibited as determined by immunoblot analysis (Figure 4c). Densitometric analyses of three independent studies demonstrated a greater than 3.5-fold increase in phospho-c-Jun ($p < .05$) in response to PACSIN1 that was blocked by silencing *Lrp1* expression (Figure 4d).

3.5 | PACSIN1 activates c-Jun in SCs in nerves after crush injury

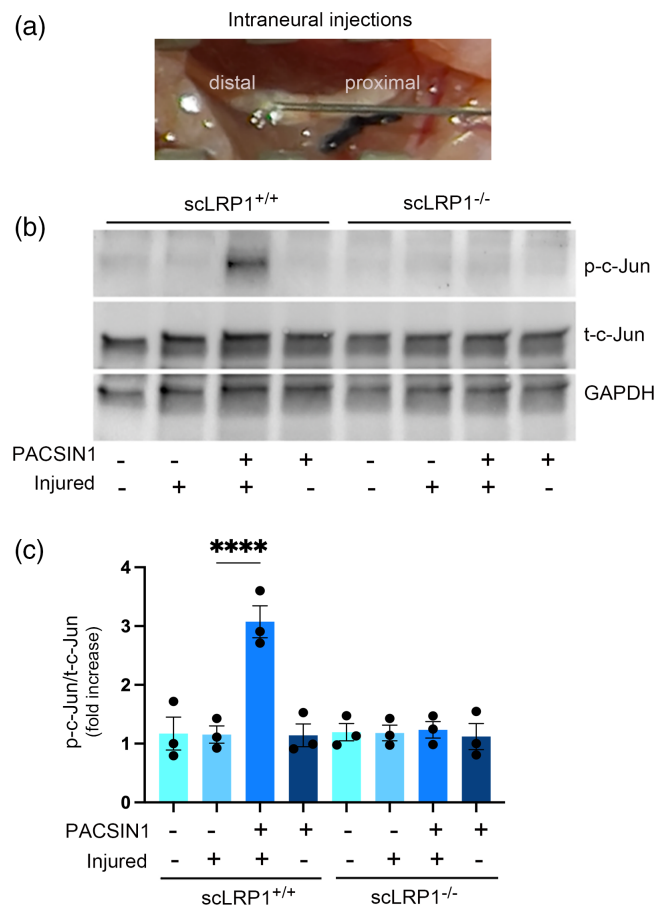To determine whether SC LRP1 is required for PACSIN1 cell signaling in injured nerves, we injected PACSIN1 (1 μM) directly into uninjured sciatic nerves and nerves distal to crush injury sites, 24 h after crush injury in scLRP1$^{+/+}$ and scLRP1$^{-/-}$ mice (Figure 5a). Nerves were harvested 15 min later. After PACSIN injection, c-Jun was only activated in injured nerves of scLRP1$^{+/+}$ mice, but not in injured nerves of scLRP1$^{-/-}$ mice (Figure 5b). Densitometric analysis demonstrated that PACSIN1 increased phospho-c-Jun by threefold when SC LRP1 was present ($p < .0001$) (Figure 5c). Phospho-c-Jun was not significantly increased by PACSIN1 in uninjured nerves in both genotypes. Further,

FIGURE 5 SC LRP1 mediates c-Jun activation by PACSIN1 in acutely injured sciatic nerves. (a) Intraneural injections of PACSIN1 in mouse sciatic nerve. (b) Transgenic mice with *Lrp1* conditionally deleted in SCs (scLRP1$^{-/-}$) and littermate controls (scLRP1$^{+/+}$) were subjected to nerve crush injury or were naive. After 24 h, nerves distal to the crush site were injected with PACSIN1 (1 μM in 2 μL) or vehicle. Nerve extracts ($n = 4$ individual mice) were subjected to immunoblot analysis to detect phospho-c-Jun or total c-Jun. (c) Immunoblots were analyzed by densitometry. The ratio of phospho-c-Jun to total-c-Jun was calculated for each treatment group. Data are expressed as mean ± SEM of three independent studies and analyzed by one-way ANOVA and Tukey's post hoc test; (****$p < .00001$ compared to uninjured and injured controls).

FIGURE 6 PACSIN1 promotes SC migration. (a) Images of SCs that migrated to the underside of Transwell membranes. Cells were treated with PACSIN1 10 nM or 25 nM, or NRG1 (0.2 nM) or vehicle (PBS). Migration was allowed to proceed for 3 h. Scale bar 200 μM. (b) Quantification of cell migration results. Data are expressed as the mean ± SEM ($n = 6$–14) and analyzed by one-way ANOVA and Tukey's post hoc test; *$p < .05$; **$p < .01$, and ****$p < .0001$ compared with vehicle control.

no differences in total c-Jun levels in scLRP1$^{+/+}$ and scLRP1$^{-/-}$ nerves were observed 24 h after injury. These results indicate that PACSIN1 is capable of acutely activating c-Jun in vivo in injured sciatic nerves.

## 3.6 | PACSIN1 induces SC migration

Ligand binding to LRP1 in SCs promotes cell migration by activating diverse cell-signaling pathways, including ERK1/2 and Rac1 (Mantuano et al., 2008, 2010). Activation of c-Jun signaling also triggers SC migration (Yamauchi et al., 2003). We tested the ability of PACSIN1 to promote SC migration using the Transwell model system (Mantuano et al., 2008). Cells were added to Transwell chambers in the Sato medium to optimize survival (Bottenstein & Sato, 1980). FBS (10%) was added to the bottom chamber. SC migration was significantly increased by PACSIN1 (25 nM) (*p* < .01) after 3 h (Figure 6a,b). NRG1 served as a positive control (Mantuano et al., 2008).

3.7 | PACSIN1 transactivates TrkC via Src family kinases

LRP1 transactivates TrkC via Src family kinases (SFKs) in sensory neurons (Yoon et al., 2013). We therefore tested whether SFKs are required for activation of c-Jun by PACSIN1. SCs were treated for 10 min with PACSIN1 with or without pretreatment with the SFK inhibitors, PP2 and AZD0530. PACSIN1 significantly activated c-Jun (approximately fourfold greater than a vehicle; *p* < .001), however, when PP2 was added, activation of c-Jun was blocked (Figure 7a,b). NT-3 also phosphorylated c-Jun. This response was not blocked by PP2, confirming that SFKs are not involved in NT-3-mediated cell signaling (Ge et al., 2020; Schecterson & Bothwell, 2010).

Because pharmacological inhibitors, including PP2, can be nonspecific, we tested whether a second pharmacological inhibitor, AZD0530 (high specificity for SFKs when used at concentrations under 20 nM; Green et al., 2009), could also regulate PACSIN1-induced c-Jun signaling. After we determined that SCs remained viable during culture with

FIGURE 7 LRP1-dependent cell-signaling initiated by PACSIN1 requires transactivation of TrkC by Src Family Kinases (SFKs) in SCs. (a, c) SCs were pretreated with PP2 (1 μM) for 15 min or AZD0530 (20 nM) for 1 hr prior to the addition of PACSIN1 (50 nM) or NT-3 (10 nM) for 10 min. Cell extracts were subjected to immunoblot analysis to detect phospho-c-Jun and total c-Jun. (b, d) Ratios of phospho-c-Jun to total-c-Jun were determined by densitometry. (e) SCs were pretreated with PP2 (1 μM) for 15 min prior to the addition of PACSIN1 (50 nM) or NT-3 (10 nM) for 10 min. Cell extracts were subjected to immunoblot analysis to detect phospho-TrkC, phospho-ERK1/2, and total ERK1/2. (f, g) Immunoblots were analyzed by densitometry. The ratios of p-TrkC or p-ERK1/2 to t-ERK1/2 were calculated for each treatment group. Data are expressed as mean ± SEM of three independent studies and analyzed by one-way ANOVA and Tukey's post hoc test; (*p* < .05; **p* < .01, ***p* < .001, and ****p* < .0001 compared to vehicle controls).
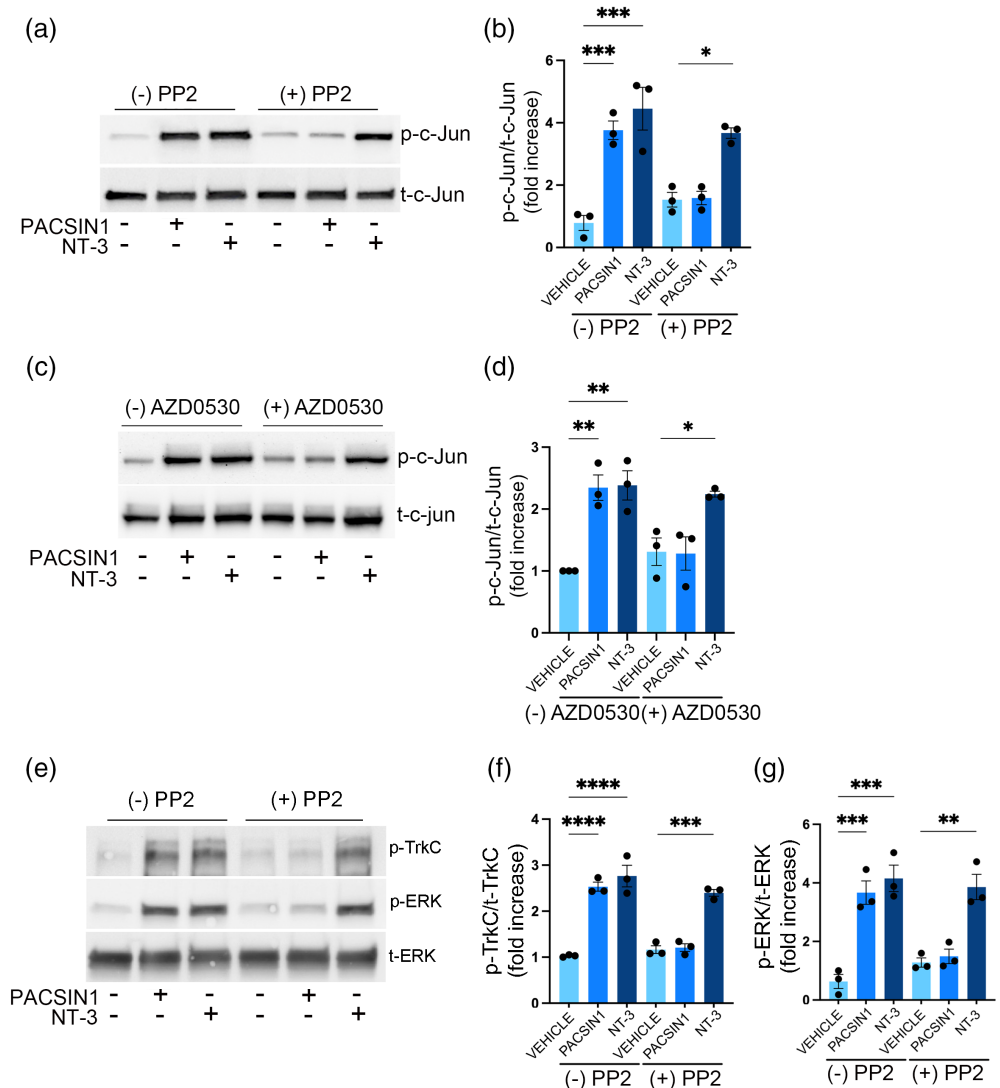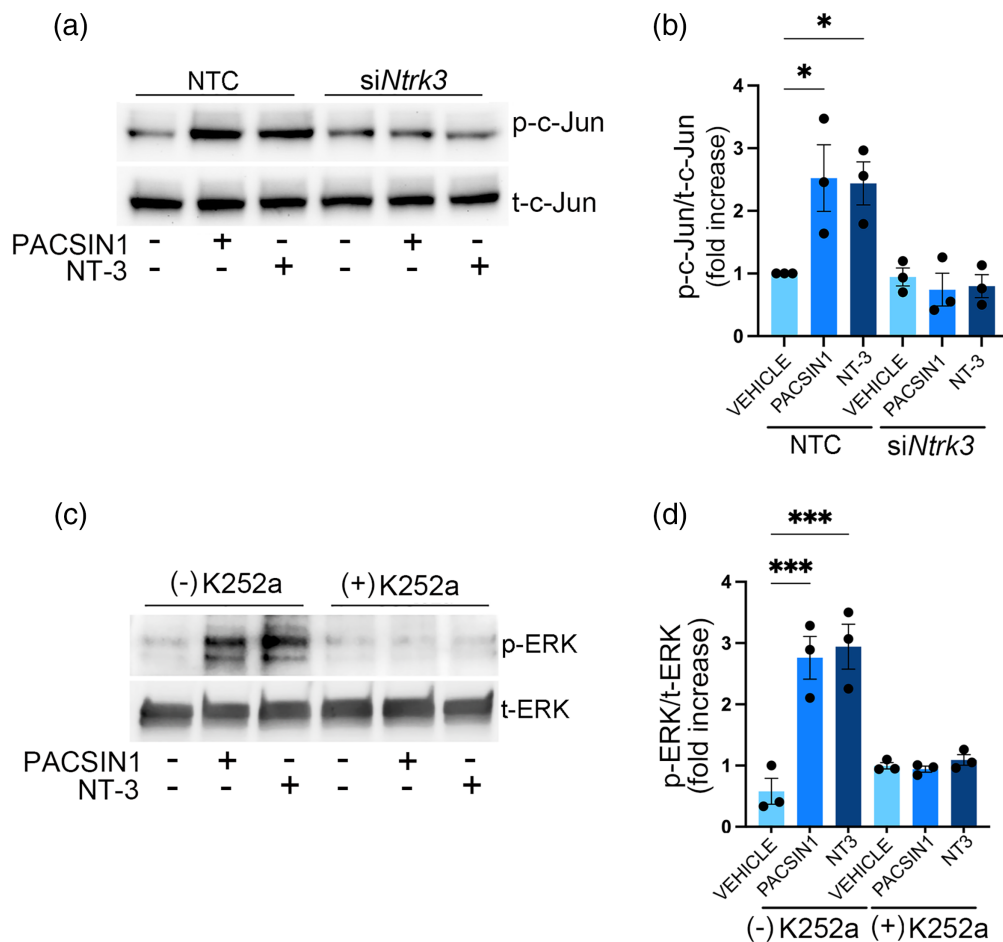
FIGURE 8 PACSIN1 requires TrkC for LRP1-dependent cell signaling. (a) SCs transiently electroporated with non-targeting control (NTC) or siRNA targeting *Ntrk3* (si*Ntrk3*) were treated with PACSIN1 (50 nM) or NT-3 (10 nM) for 10 min. Cell extracts were subjected to immunoblot analysis to detect phospho-c-Jun and total c-Jun. (b) Immunoblots were analyzed by densitometry. The ratios of p-c-Jun to t-c-Jun were calculated for each treatment group. (c) SCs were pre-treated with K252a (100 nM) for 30 min prior to the addition of PACSIN1 (50 nM) or NT-3 (10 nM) for 10 min. Cell extracts were subjected to immunoblot analysis to detect phospho-ERK1/2 and total-ERK1/2. (d) Immunoblots were analyzed by densitometry. Ratios of phospho-ERK1/2 to total ERK1/2 were calculated for each treatment group. Data are expressed as mean ± SEM of three independent studies and analyzed by one-way ANOVA and Tukey's post hoc test; (*$p < .05$; ***$p < .001$, compared to vehicle controls).

AZD0530 up to 100 nM (Figure 2s), the cells were pretreated with AZD0530 (20 nM) for 1 h, and subsequently, PACSIN1 or NT-3 was added to the cultures for 10 min. Both PACSIN1 and NT-3 induced phosphorylation of c-Jun (Figure 7c,d; $p < .01$). However, AZD0530 blocked PACSIN1-induced c-Jun phosphorylation, but not NT-3-induced c-Jun phosphorylation (Figure 7c,d; $p < .05$), suggesting that c-Jun activation occurs downstream of SFKs when PACSIN1 binds to LRP1.

Next, we investigated whether the SC-specific receptor tyrosine kinase, TrkC, is transactivated by SFKs in response to PACSIN1. Schwann cells were pretreated with PP2, and subsequently, PACSIN1 or NT-3 was added to the cultures for 10 min. Both PACSIN1 and NT-3 induced phosphorylation of TrkC (Figure 7e,f; $p < .001$). PP2 blocked PACSIN1-induced TrkC phosphorylation, but not NT-3-induced TrkC phosphorylation ($p < .01$). PP2 also blocked ERK1/2 activation in PACSIN1-treated cells, but not in NT-3-treated cells

(Figure 7e,g; $p < .05$), suggesting that ERK1/2 activation occurs downstream of SFKs when PACSIN1 binds to LRP1.

When *Ntrk3* gene expression (TrkC) was silenced with siRNA, the mRNA levels of the *Ntrk3* were significantly decreased (>85%), as determined by RT-qPCR (Figure S3A; $p < .01$). In contrast, *Ntrk2* (TrkB) was not changed (Figure S3B) demonstrating the specificity of *Ntrk3* silencing in SCs. In TrkC-deficient SCs, PACSIN1 failed to induce c-Jun phosphorylation compared to NTC control SCs (Figure 8a; $p < .05$). NT-3 did not signal in TrkC-deficient SCs, as anticipated. Densitometric analyses of three independent studies demonstrated a greater than two-fold increase in phospho-c-Jun (Figure 8b; $p < .05$) in response to PACSIN1 or NT-3 that was blocked when *Ntrk3* was silenced.

Finally, we performed pharmacological inhibitory studies using the Trk inhibitor, K252a. Pretreatment with K252a blocked PACSIN1 activation of ERK1/2 (Figure 8c,d), indicating that Trk receptor
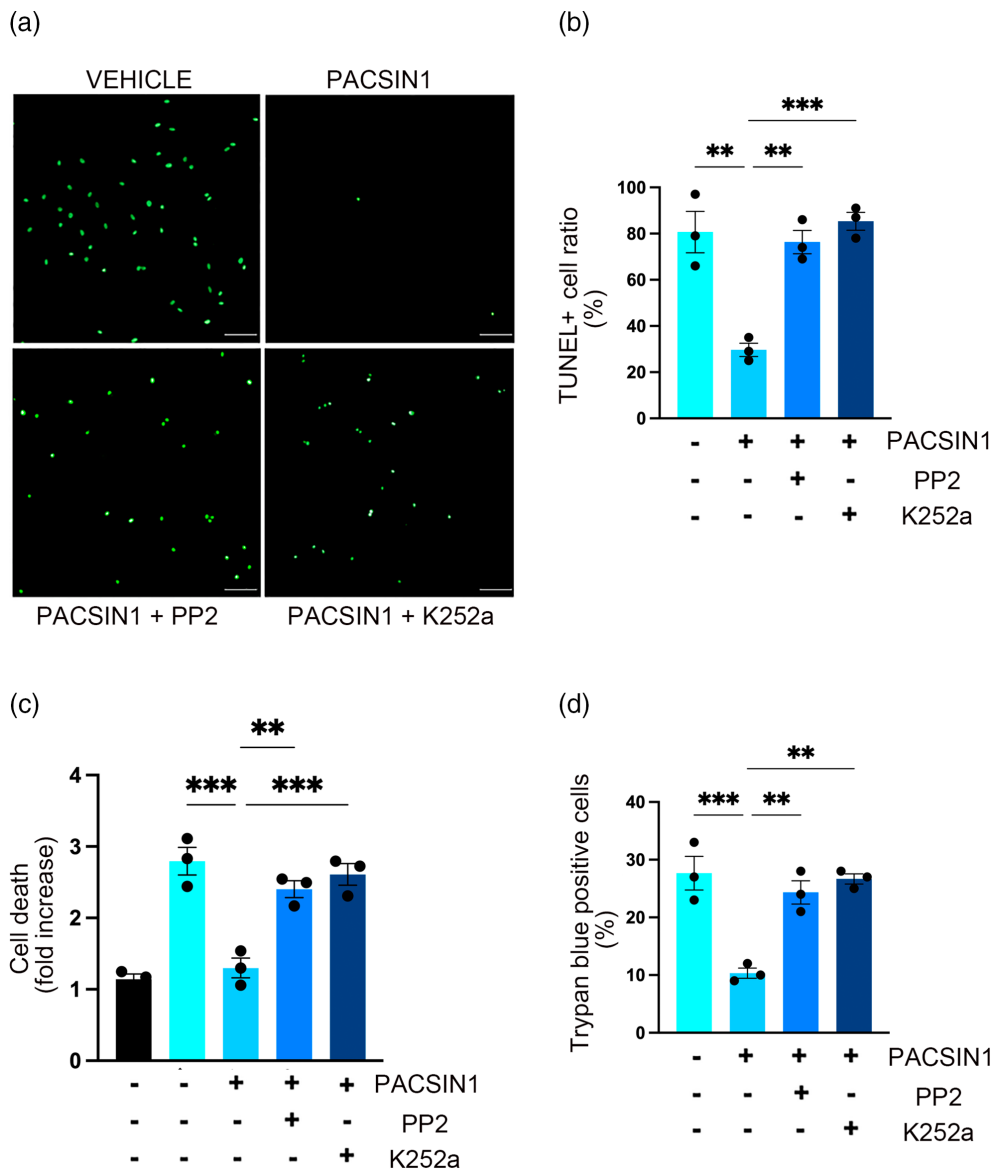
FIGURE 9 Transactivation of TrkC is essential for PACSIN1-induced SC survival. (a) SCs were pretreated with PP2 (1 μM) or K252a (100 nM) for 90 min prior to the addition of PACSIN1 (50 nM). After 6 h, SCs were fixed and labeled with TUNEL. Representative immunofluorescence images of TUNEL+ SCs (green) demonstrate that PACSIN prevents apoptosis. Scale bar 500 μM. (b) Quantification of TUNEL+ SCs compared with total PI/RNase-stained SC nuclei. (c) SCs were pretreated with PP2 (1 μM) or K252a (100 nM) for 90 min prior to the addition of PACSIN1 (50 nM) in a low serum medium. After 18 h, SC oligonucleosomes were measured by the Cell Death ELISA™. Results are shown as a "fold increase in SC death" compared with SCs cultured in 10% FBS (black column). (d) SCs were pretreated with PP2 (1 μM) or K252a (100 nM) for 90 min prior to the addition of PACSIN1 (50 nM). After 18 h, SCs were stained with Trypan blue. Clear and blue stained cytoplasm in cells were counted. Results are expressed as % of Trypan blue (dead cells). Data are expressed as mean ± SEM of three independent studies and analyzed by one-way ANOVA and Tukey's post hoc test; (**$p < .01$, ***$p < .001$, ****$p < .0001$ compared to PACSIN1 treated cells).

phosphorylation is required for downstream SC repair signaling. Collectively, these results indicate that TrkC transactivation by SFKs is required for the complete continuum of PACSIN1/LRP1-dependent cell-signaling events associated with the SC Repair Program.

3.8 | PACSIN1 promotes SC survival

To test whether PACSIN1-induced TrkC transactivation promotes SC survival, we applied several different approaches. First, we examined

apoptosis. We exposed cultured SCs to a low serum medium (0.5% FBS) and observed a significant fraction (80 ± 8% of total cells) of TUNEL-positive (apoptotic) cells within 6 h (Figure 9a,b). In contrast, no TUNEL-positive cells were observed in SC cultured in 10% FBS (data not shown). SCs cultured in 0.5% FBS and PACSIN1 demonstrated significantly lower TUNEL positivity (25% of total cells; $p < .01$). When SCs were briefly exposed (90 min) to PP2 (1 μM) or K252a (100 nM) prior to the addition of PACSIN1, TUNEL positivity reverted to the level observed when PACSIN1 was not added.

(a)

(b)

(c)

FIGURE 10 PACSIN1 regulates the expression of SC genes that are associated with SC phenotypic change in the response to injury. SCs were serum-starved for approximately 1 h to elevate levels of LRP1 prior to the addition of PACSIN1 (50 nM) or vehicle for 5 h (a). Hierarchical clustering and heat map analysis of differentially expressed genes (48 genes) are shown. The scaled expression value (row Z score) is shown in a blue-red color scheme with red indicating higher expression and blue indicating lower expression. (b) Volcano plot showing fold changes in gene expression that are also statistically significant at the adjusted $p < .4$ level. Increases or decreases are labeled in red or blue, respectively. Gray points are not significant. RNASeq data represent 3–4 independent biological replicates per group. (c) Validation of key differentially regulated genes by RT-qPCR including *ARID4B*, *Egr1*, and *VCAN* gene expression. Data are expressed as mean ± SEM of three independent studies and analyzed by *T*-test; (*$p < .05$; **$p < .01$, ****$p < .0001$).

Next, we measured oligonucleosomes, as an early indicator of cell death using the Cell Death ELISA kit™. Previously, we demonstrated that SCs cultured in 0.5% FBS containing media display 3-fold increased cell death compared with SCs cultured for 18 h in 10% FBS (Sadri et al., 2022) and consistent with our data herein (Figure 9c). SCs cultured with PACSIN1 in 0.5% FBS media showed significantly reduced cell death ($p < .001$). When SCs were briefly exposed (90 min) to PP2 (1 μM) or K252a (100 nM) prior to the

addition of PACSIN1, the pro-survival effects of PACSIN1 were blocked (Figure 9c).

Finally, we measured necrotic cell death by Trypan blue exclusion. When SCs were cultured in 0.5% FBS, 28% of the cells demonstrated Trypan blue uptake, suggesting cell death. By contrast, SCs cultured in 0.5% FBS and PACSIN1 had decreased levels of cell death; 10% of counted cells took up Trypan blue after 18 h (Figure 9d; $p < .001$). When SCs were briefly exposed (90 min) to PP2 (1 μM) or K252a

(100 nM), prior to the addition of PACSIN1, the pro-survival effects of PACSIN1 were inhibited; levels of cell death rose to approximately 25%–27% with either treatment. Collectively, these results support the role of PACSIN1 as a potent SC survival factor and are consistent with the known SC survival role of SC LRP1 (Campana et al., 2006).

3.9 | PACSIN1 promotes changes in early injury-induced gene expression in SCs

We compared the SC transcriptome in vehicle- and PACSIN1-treated SCs in culture. A total of 48 differentially regulated genes were identified, as shown in the heat map and volcano plot (Figure 10a,b). The data have been submitted to Figshare (https://figshare.com/s/6bc1bb1e4f25a49fc062), a public database. Many of the regulated genes are previously identified as playing a role in the response to nerve injury and repair. For example, *Ccnd1* (cyclin D1), which controls cell cycle dynamics and is required for SC growth and the repair phenotype (Kim et al., 2000; Yun et al., 2010), was significantly upregulated (adjusted *p* < .028).

The effects of PACSIN1 on *ARID4B*, *Egr1*, and *VCAN* gene expression were validated by qPCR (Figure 10c). ARID4B is an extracellular matrix protein that inhibits nerve regeneration (Warren et al., 2020). PACSIN1 significantly down-regulated *ARID4B* in SCs. PACSIN1 up-regulated expression of the transcription factor *Egr1*, which is expressed primarily in early-stage SCs and negatively regulates myelination (Khodabakhsh et al., 2021; Topilko et al., 1997). Furthermore, PACSIN1 significantly up-regulated versican (*VCAN*), a major component of the extracellular matrix that is required for appropriate clustering of sodium channels at the Node of Ranvier (Dours-Zimmermann et al., 2009). Collectively, these findings may support a role for PACSIN1 in the activation and sustaining of the SC Repair Program.

4 | DISCUSSION

In this study, we demonstrated for the first time that a protein is released by injured axons in the PNS and is capable of triggering LRP1-dependent cell-signaling in support of the SC Repair Program. While LRP1 ligands have been previously reported to promote elements of the SC Repair Program (Flütsch et al., 2016; Mantuano et al., 2008; Mantuano et al., 2015), in the present study, a novel, endogenous LRP1 ligand, PACSIN1, previously identified as an intracellular neuronal protein in the CNS, revealed itself as an extracellular mediator of SC LRP1-dependent cell signaling, survival and migration. Our evidence implicates PACSIN1 as a likely early driver of LRP1 cell-signaling in the PNS. Accordingly, PACSIN1 activated c-Jun in vivo in sciatic nerves only when the nerves were recently injured and only in mice that express SC LRP1. Responses were not observed in scLRP1$^{-/-}$ mice, implicating SC LRP1 as the exclusive PACSIN1 target. Because PACSIN1 was active only after sciatic nerve injury, probably due to the up-regulation of SC LRP1 expression (Campana

et al., 2006), it is likely that the PACSIN1/LRP1 interaction supports and sustains the SC Repair Program as opposed to initiating it.

LRP1 binds over 100 structurally diverse ligands, including proteins released by injured and dying cells, which enables this receptor to recognize tissue injury and mediate appropriate cellular responses (Fernandez-Castaneda et al., 2013; Gonias & Campana, 2014; Strickland et al., 2002). Not all LRP1 ligands activate cell signaling and there is evidence that the signaling pathways activated may be ligand-dependent (Mantuano et al., 2013) and have distinct co-receptors (Mantuano et al., 2022; Rohrbach et al., 2021). The LRP1 ligand characterized herein, PACSIN1, is an F-BAR and SH3-domain containing protein with established roles in endocytosis of the transferrin and AMPA receptors (Widagdo et al., 2016). PACSIN1, also termed syndaptin 1, plays a key role in the presynaptic compartments of neurons, supporting receptor trafficking, neurotransmitter recycling, and synaptic plasticity (Dumont & Lehtonen, 2022; Schael et al., 2013; Widagdo et al., 2016). In the brain, PACSIN1 regulates cytoskeletal networks (Qualmann & Kelly, 2000). Recently, a mouse model with a global knockout of Syndapin 1/PACSIN1 was developed and characterized (Koch et al., 2020). These mice have significant defects in NMDA-R function, that are characterized by GluA1/2 heterodimer disorganization, aberrant trafficking, and function. Loss of PACSIN1 was associated with increases in schizophrenia-like behaviors and synaptic dysfunction. Whether PACSIN1 deletion in primary sensory neurons would replicate scLRP1$^{-/-}$ mice after injury is not certain. While the axon-derived PACSIN1-SC LRP1 interaction would be lost and SC repair signaling would be compromised, it is possible that compensatory LRP1 ligands in the injured nerve environment could replicate some cell signaling activities. Indeed, other known LRP1 ligands such as plasma-derived alpha-2-macroglobulin (Gonias et al., 1983) and decorin are present in the extracellular nerve spaces and are capable of inducing LRP1-dependent cell signaling. Axon-derived PACSIN1, which may be an early activator of SC LRP1 given its proximity, may be part of a continuum of endogenous LRP1 ligands contributing to a truly effective SC Repair Program. In addition, PACSIN1 is a multifaceted protein that has an intrinsic function in neurons, that is separate from the newly discovered extracellular activities of LRP1-dependent cell signaling which could complicate data interpretation in a PACSIN1 knock-out mouse. Nonetheless, studies identifying which types of sensory neurons abundantly express PACSIN1, and their contribution to functional nerve repair will be important future studies.

Previous work demonstrated that PACSIN1 was abundantly present in cultured DRG neurons (Liu et al., 2012), consistent with our studies showing immunoreactivity of PACSIN1 in both small and large-diameter neurons in DRGs in vivo. Similar to the neuron-specific localization of PACSIN1 in the CNS, we identified PACSIN1 immunoreactivity exclusively in cell bodies and axons of DRG neurons. Our finding that PACSIN1 is located in the extracellular spaces of injured nerves confirms that it is released from injured axons. Although LRP1 is ubiquitously expressed in many cell types, LRP1 is acutely up-regulated after injury or stress in SCs and is unchanged in expression in DRG neurons (Campana et al., 2006). The physical proximity of released PACSIN1 to SC LRP1 supports a model in which these two

gene products play an important role in SC-sensory neuron communication during injury. We hypothesize that a lack of PACSIN1 in primary sensory neurons would contribute to a less-than-optimal SC LRP1 response in transitioning to an SC repair phenotype after injury.

LRP1 ligands activate cell signaling by interacting with a receptor assembly that frequently includes the ionotropic glutamate receptor, the NMDA-R (Mantuano et al., 2013, 2015). We demonstrated that the NMDA-R is essential for SC signaling in response to PACSIN1 in experiments with the NMDA-R channel inhibitor, MK-801. The function of the NMDA-R as a receptor in SCs that responds to proteins is fairly new (Campana et al., 2017; Mantuano et al., 2015). However, when LRP1 ligands such as α_2M engage the NMDA-R, calcium flux is altered (Qiu et al., 2002), and this activates SFKs (Rusanescu et al., 1995). SFKs phosphorylate the LRP1 cytoplasmic tail which serves as a scaffold for signaling proteins (Bilodeau et al., 2010; Herz & Strickland, 2001; Luo et al., 2018) and, in addition, can transactivate receptor tyrosine kinases (RTKs) such as Trk receptors (Shi et al., 2009). When RTKs are transactivated, downstream cell-signaling factors are phosphorylated as if the RTK engaged its primary ligand. In this study, we show that the RTK, TrkC, which is specifically localized to SCs and small diameter neurons in the DRG (Hess et al., 2007; Yoon et al., 2013), is transactivated by SFKs after PACSIN1 engages LRP1 in primary cultured SCs. Our findings are consistent with our previously described data showing transactivation of TrkC by known LRP1 ligands in primary sensory neurons (Yoon et al., 2013). In SCs, this transactivation mechanism appears to be an important step in LRP1 signaling and may be essential to activate the complete continuum of SC LRP1 signaling after PNS injury.

Interestingly, after sciatic nerve injury, both LRP1 and TrkC are up-regulated in SCs within 24 h (Campana et al., 2006; Funakoshi et al., 1993), however, the ligand for TrkC, NT-3, is not up-regulated and in fact decreases significantly after PNS injury. These results suggest that in PNS injury, high levels of TrkC may serve mainly as transactivation targets as opposed to receptors for directly binding ligands. Further studies elucidating the temporal activation of TrkC in sciatic nerves after injury are needed. Transactivation of TrkC receptors has been previously observed in developing neuronal systems. For example, epidermal growth factor receptor transactivates TrkC in cortical precursor cells during development when the TrkC ligands, BDNF and NT-3, are not present in the local microenvironment (Puehringer et al., 2013). LRP1 emerges as an orchestrator of distinct cell-signaling pathways that modulate SC survival and changes in phenotype in injury.

Previous studies from our group characterized the functional consequences of LRP1-dependent cell signaling (Mantuano et al., 2008; Mantuano et al., 2011). Schwann cell survival and migration are key features of the SC Repair Program (Min et al., 2021) and these activities can be mediated by LRP1. There is accumulating evidence that regenerating axons are unable to cross a nerve gap in the absence of significant SC engagement. Elegant studies performed by Cattin et al. (2015) demonstrated that SCs migrate on newly formed blood vessels after injury and are part of an organized migration unit. Migrating SCs form SC cords in the nerve gap and carry axons with them from the proximal nerve stump into the distal nerve stump (Chen et al., 2019). From a therapeutic viewpoint, early and increased survival as well as efficiency of SC migration after PNS injury may provide a more cohesive microenvironment for axon regrowth and thus, dictate the success of peripheral nerve regeneration. We demonstrated that LRP1-induced SC survival and migration are mediated by the cell-signaling factors: ERK1/2; PI3K/Akt; and Rac1 (Mantuano et al., 2008, 2010). We now understand that c-Jun is activated downstream of TrkC in cells treated with an LRP1 ligand. It is thus, plausible that activation of c-Jun is involved in LRP1-promoted SC migration. Activation of c-Jun terminal kinase (JNK) downstream of NT-3 and TrkC has been previously associated with increased SC migration (Yamauchi et al., 2003).

PACSIN1 regulated the SC transcriptome. By comparing the SC transcriptome in vehicle- and PACSIN1-treated SCs, we identified 48 differentially regulated genes, many of which are previously identified as genes that promote SC phenotypic change in peripheral nerve injury. We noted a smaller than anticipated number of differentially regulated genes between the groups; however, this may be due to the short time period of PACSIN1 exposure (5 h). When we compared PACSIN1-induced gene expression in primary cultured rat SCs to gene expression in SCs isolated from day 3 post-crush injured rat nerves (Brosius Lutz et al., 2022), we detected 89.8% of the same differentially regulated genes. Of the top five upregulated genes after PACSIN1 treatment, three of the genes were also significantly upregulated in day 3 post-crush injured rat nerves. Of the top five down-regulated genes after PACSIN1 treatment, three were downregulated in day 3 post-crush injured rat nerves. Collectively, these findings suggest that PACSIN1-induced gene expression is consistent, at least in part, with genes expressed in SCs early in nerve injury, although a relationship to c-Jun activation has not been formally demonstrated.

One of the top upregulated genes was *Ccnd1*, which encodes cyclin D1. Cyclin D1 has been extensively studied in SCs and is essential to the growth of mature SCs (Atanasoski et al., 2001; Kim et al., 2000). *Ccnd*1 was also significantly upregulated in isolated SCs three days after crush injury (Brosius Lutz et al., 2022). Mature SCs selectively utilize cyclin D1 for cell growth and other cyclins (D2, D3) cannot compensate for its activities (Kim et al., 2000). Cyclin D1 facilitates the phenotypic transition of SCs. Moreover, in the adult mouse, cyclin D1 promotes SC proliferation and is responsible for the generation of excess SCs to ensure sufficient numbers of SCs for the organization of nerve repair. Newly generated SCs undergo apoptosis. In cyclin D1 knock-out mice, pre-existing SCs in the distal stump do not divide (Yang et al., 2008). Our data demonstrating that PACSIN1 significantly upregulated *ccnd1* in SCs may partially explain the effects of PACSIN1 on SC survival. We validated 3 other genes by RT-qPCR including the transcription factor, *Egr1*. *Egr1* and *Egr3* are injury-related signals in peripheral nerves including regulation of p75^{NTR} in SCs (Gao et al., 2007; Nikam et al., 1995). Upregulation of p75^{NTR} is a key function for transitioning SCs to a repair phenotype. *Egr1* is also known as an early-stage SC differentiation marker (Khodabakhsh et al., 2021; Topilko et al., 1997). In primary SCs, PACSIN1 significantly upregulated *Egr1* which is consistent with facilitating the SC Repair Program.

PACSIN1 may regulate the composition of the extracellular matrix by increasing or decreasing the expression of key regeneration-associated extracellular matrix genes. Chondroitin sulfate proteoglycan, *ARID4B* expression, which is known to inhibit nerve regeneration (Warren et al., 2020) was antagonized by PACSIN1 stimulation. PACSIN1 significantly up-regulated versican (*VCAN*), a major component of the extracellular matrix that participates in adhesion, proliferation, and migration (Paulus et al., 1996) and is often simultaneously up-regulated with *Egr1* (Ye et al., 2016). The up-regulation of this extracellular matrix protein may support the pro-migratory effects we observed by PACSIN1. Furthermore, *VCAN* was significantly upregulated in isolated SCs collected 3 days after nerve crush injury (Brosius Lutz et al., 2022). Notably, PACSIN1 significantly upregulated Cox7ac, a cytochrome c-oxidase subunit, important in mitochondrial bioenergetics, that was also upregulated in SCs from early injured nerves (Brosius Lutz et al., 2022). Collectively, our transcriptome profiling results suggest that PACSIN1 induces gene expression in cultured SCs similar to genes expressed early after nerve injury, and could play a role in facilitating the SC Repair Program.

In conclusion, our findings demonstrate for the first time that PACSIN1, a novel axon-derived protein, is a functional LRP1 agonist. By engaging LRP1, PACSIN1 activates SC Repair signaling via a mechanism in which SFKs transactivate the receptor tyrosine kinase, TrkC. To our knowledge, this is the first time that an intracellular protein has been shown to function as an activator of LRP1 cell-signaling to facilitate the response to peripheral nerve injury. These findings highlight the importance of axon-SC communication during injury.

AUTHOR CONTRIBUTIONS

S.M., A.F., M.C., M.N, D.P., E.M., M.S., Z.W. and P.A. conducted the experiments; D.C-F., and S.B.R. analyzed the RNA-Seq data; S.M. and W.M.C. wrote the manuscript; S.L.G. and W.M.C. edited the manuscript. All authors participated in the experiment design and results interpretation, and edited and approved the final draft of the manuscript.

ACKNOWLEDGMENTS

DATA AVAILABILITY STATEMENT

The raw LC-MS/MS and Bulk RNA-Seq files for the characterization of samples are available and browsable in the public repository in Figshare (https://figshare.com/s/6bc1bb1e4f25a49fc062).

ORCID

Stefano Martellucci (ID) https://orcid.org/0000-0002-3952-3162
Wendy M. Campana (ID) https://orcid.org/0000-0002-9039-1396

REFERENCES

Akassoglou, K., Yu, W. M., Akpinar, P., & Strickland, S. (2002). Fibrin inhibits peripheral nerve remyelination by regulating Schwann cell differentiation. *Neuron*, 33(6), 861–875. https://doi.org/10.1016/s0896-6273(02)00617-7

Andrews, S. (2010). FastQC: A quality control tool for high throughput sequence data [online]. http://www.bioinformatics.babraham.ac.uk/projects/fastqc/

Arthur-Farraj, P. J., Latouche, M., Wilton, D. K., Quintes, S., Chabrol, E., Banerjee, A., Woodhoo, A., Jenkins, B., Rahman, M., Turmaine, M., Wicher, G. K., Mitter, R., Greensmith, L., Behrens, A., Raivich, G., Mirsky, R., & Jessen, K. R. (2012). c-Jun reprograms Schwann cells of injured nerves to generate a repair cell essential for regeneration. *Neuron*, 75(4), 633–647. https://doi.org/10.1016/j.neuron.2012.06.021

Atanasoski, S., Shumas, S., Dickson, C., Scherer, S. S., & Suter, U. (2001). Differential cyclin D1 requirements of proliferating Schwann cells during development and after injury. *Molecular and Cellular Neurosciences*, 18(6), 581–592. https://doi.org/10.1006/mcne.2001.1055

Azzouz, M., Kenel, P. F., Warter, J.-M., Poindron, P., & Borg, J. (1996). Enhancement of mouse sciatic nerve regeneration by the long chain fatty alcohol, N-Hexacosanol. *Experimental Neurology*, 138(2), 189–197. https://doi.org/10.1006/exnr.1996.0057

Benjamini, Y., & Hochberg, Y. (1995). Controlling the false discovery rate: A practical and powerful approach to multiple testing. *Journal of the Royal Statistical Society. Series B, Statistical Methodology*, 1(57), 289–300. https://doi.org/10.1111/j.2517-6161.1995.tb02031.x

Bilodeau, N., Fiset, A., Boulanger, M. C., Bhardwaj, S., Winstall, E., Lavoie, J. N., & Faure, R. L. (2010). Proteomic analysis of Src family kinases signaling complexes in Golgi/endosomal fractions using a site-selective anti-phosphotyrosine antibody: Identification of LRP1-insulin receptor complexes. *Journal of Proteome Research*, 9(2), 708–717. https://doi.org/10.1021/pr900481b

Bolger, A. M., Lohse, M., & Usadel, B. (2014). Trimmomatic: A flexible trimmer for Illumina sequence data. *Bioinformatics*, 30(15), 2114–2120. https://doi.org/10.1093/bioinformatics/btu170

Boll, E., Cantrelle, F. X., Landrieu, I., Hirel, M., Sinnaeve, D., & Levy, G. (2020). 1H, 13C, and 15N chemical shift assignment of human PACSIN1/syndapin I SH3 domain in solution. *Biomolecular NMR Assignments*, 14(2), 175–178. https://doi.org/10.1007/s12104-020-09940-z

Bottenstein, J. E., & Sato, G. H. (1980). Fibronectin and polylysine requirement for proliferation of neuroblastoma cells in defined medium. *Experimental Cell Research*, 129(2), 361–366. https://doi.org/10.1016/0014-4827(80)90504-2

Brosius Lutz, A., Lucas, T. A., Carson, G. A., Caneda, C., Zhou, L., Barres, B. A., Buckwalter, M. S., & Sloan, S. A. (2022). An RNA-sequencing transcriptome of the rodent Schwann cell response to peripheral nerve injury. *Journal of Neuroinflammation*, 19(1), 105. https://doi.org/10.1186/s12974-022-02462-6

Campana, W. M., Li, X., Dragojlovic, N., Janes, J., Gaultier, A., & Gonias, S. L. (2006). The low-density lipoprotein receptor-related protein is a pro-survival receptor in Schwann cells: Possible implications in peripheral nerve injury. *The Journal of Neuroscience*, 26, 11197–11207. https://doi.org/10.1523/JNEUROSCI.2709-06.2006

Campana, W. M., Mantuano, E., Azmoon, P., Henry, K., Banki, M. A., Kim, J. H., Pizzo, D. P., & Gonias, S. L. (2017). Ionotropic glutamate receptors activate cell signaling in response to glutamate in Schwann cells. *The FASEB Journal*, 31(4), 1744–1755. https://doi.org/10.1096/fj.201601121R

Cattin, A. L., Burden, J. J., Van Emmenis, L., Mackenzie, F. E., Hoving, J. J., Garcia Calavia, N., et al. (2015). Macrophage-induced blood vessels guide Schwann cell-mediated regeneration of peripheral nerves. *Cell*, 162(5), 1127–1139. https://doi.org/10.1016/j.cell.2015.07.021

Chen, B., Chen, Q., Parkinson, D. B., & Dun, X. P. (2019). Analysis of Schwann cell migration and axon regeneration following nerve injury

in the sciatic nerve bridge. _Frontiers in Molecular Neuroscience_, _12_(308), 2019. https://doi.org/10.3389/fnmol.2019.00308.eCollection

Dobin, A., Davis, C. A., Schlesinger, F., Drenkow, J., Zaleski, C., Jha, S., Batut, P., Chaisson, M., & Gingeras, T. R. (2013). STAR: ultrafast universal RNA-seq aligner. _Bioinformatics_, _29_(1), 15–21. https://doi.org/10.1093/bioinformatics/bts635

Dours-Zimmermann, M. T., Maurer, K., Rauch, U., Stoffel, W., Fässler, R., & Zimmermann, D. R. (2009). Versican V2 assembles the extracellular matrix surrounding the nodes of Ranvier in the CNS. _The Journal of Neuroscience_, _29_(24), 7731–7742. https://doi.org/10.1523/JNEUROSCI.4158-08.2009

Dumont, V., & Lehtonen, S. (2022). PACSIN proteins in vivo: Roles in development and physiology. _Acta Physiologica (Oxford, England)_, _234_(3), e13783. https://doi.org/10.1111/apha.13783

El-Horany, H. E., Watany, M. M., Hagag, R. Y., El-Attar, S. H., & Basiouny, M. A. (2019). Expression of LRP1 and CHOP genes associated with peripheral neuropathy in type 2 diabetes mellitus: Correlations with nerve conduction studies. _Gene_, _702_, 114–122. https://doi.org/10.1016/j.gene.2019.02.105

Feltri, M. L., D'antonio, M., Quattrini, A., Numerato, R., Arona, M., Previtali, S., et al. (1999). A novel P0 glycoprotein transgene activates expression of lacZ in myelin-forming Schwann cells. _The European Journal of Neuroscience_, _11_(5), 1577–1586. https://doi.org/10.1046/j.1460-9568.1999.00568.x

Feltri, M. L., Graus Porta, D., Previtali, S. C., Nodari, A., Migliavacca, B., Cassetti, A., et al. (2002). Conditional disruption of beta 1 integrin in Schwann cells impedes interactions with axons. _The Journal of Cell Biology_, _156_(1), 199–209. https://doi.org/10.1083/jcb.200109021

Fernandez-Castaneda, A., Arandjelovic, S., Stiles, T. L., Schlobach, R. K., Mowen, K. A., Gonias, S. L., & Gaultier, A. (2013). Identification of the low density lipoprotein (LDL) receptor-related protein-1 interactome in central nervous system myelin suggests a role in the clearance of necrotic cell debris. _The Journal of Biological Chemistry_, _288_(7), 4538–4548. https://doi.org/10.1074/jbc.M112.384693

Flütsch, A., Henry, K., Mantuano, E., Lam, M. S., Shibayama, M., Takahashi, K., Gonias, S. L., & Campana, W. M. (2016). Evidence that LDL-receptor-related protein 1 (LRP1) acts as an early injury detection receptor and activates c-Jun in Schwann cells. _NeuroReport_, _27_, 1305–1311. https://doi.org/10.1097/WNR.0000000000000691

Funakoshi, H., Frisén, J., Barbany, G., Timmusk, T., Zachrisson, O., Verge, V. M., & Persson, H. (1993). Differential expression of mRNAs for neurotrophins and their receptors after axotomy of the sciatic nerve. _The Journal of Cell Biology_, _123_(2), 455–465. https://doi.org/10.1083/jcb.123.2.455

Gao, X., Daugherty, R. L., & Tourtellotte, W. G. (2007). Regulation of low affinity neurotrophin receptor (p75(NTR)) by early growth response (Egr) transcriptional regulators. _Molecular and Cellular Neurosciences_, _36_(4), 501–514. https://doi.org/10.1016/j.mcn.2007.08.013

Garcia-Fernandez, P., Uceyler, N., & Sommer, C. (2021). From the low-density lipoprotein receptor-related protein 1 to neuropathic pain: A potentially novel target. _Pain Report_, _6_(1), e898. https://doi.org/10.1097/PR9.0000000000000898

Gaultier, A., Simon, G., Niessen, S., Dix, M., Takimoto, S., Cravatt, B. F., 3rd, et al. (2010). LDL receptor-related protein 1 regulates the abundance of diverse cell-signaling proteins in the plasma membrane proteome. _Journal of Proteome Research_, _9_(12), 6689–6695. https://doi.org/10.1021/pr1008288

Ge, M. M., Zhou, Y. Q., Tian, X. B., Manyande, A., Tian, Y. K., Ye, D. W., & Yang, H. (2020). Src-family protein tyrosine kinases: A promising target for treating chronic pain. _Biomedicine & Pharmacotherapy_, _125_, 110017. https://doi.org/10.1016/j.biopha.2020.110017

Gonias, S. L., Balber, A. E., Hubbard, W. J., & Pizzo, S. V. (1983). Ligand binding, conformational change and plasma elimination of human, mouse and rat alpha-macroglobulin proteinase inhibitors. _The Biochemical Journal_, _209_(1), 99–105. https://doi.org/10.1042/bj2090099

Gonias, S. L., & Campana, W. M. (2014). LDL receptor-related protein-1: A regulator of inflammation in atherosclerosis, cancer, and injury to the nervous system. _The American Journal of Pathology_, _184_(1), 18–27. https://doi.org/10.1016/j.ajpath.2013.08.029

Green, T. P., Fennell, M., Whittaker, R., Curwen, J., Jacobs, V., Allen, J., Logie, A., Hargreaves, J., Hickinson, D. M., Wilkinson, R. W., Elvin, P., Boyer, B., Carragher, N., Plé, P. A., Bermingham, A., Holdgate, G. A., Ward, W. H. J., Hennequin, L. F., Davies, B. R., & Costello, G. F. (2009). Preclinical anticancer activity of the potent, oral Src inhibitor AZD0530. _Molecular Oncology_, _3_(3), 248–261. https://doi.org/10.1016/j.molonc.2009.01.002

Grimm-Günter, E. M., Milbrandt, M., Merkl, B., Paulsson, M., & Plomann, M. (2008). PACSIN proteins bind tubulin and promote microtubule assembly. _Experimental Cell Research_, _314_(10), 1991–2003. https://doi.org/10.1016/j.yexcr.2008.03.015

Heiman, M., Schaefer, A., Gong, S., Peterson, J. D., Day, M., Ramsey, K. E., Suárez-Fariñas, M., Schwarz, C., Stephan, D. A., Surmeier, D. J., Greengard, P., & Heintz, N. (2008). A translational profiling approach for the molecular characterization of CNS cell types. _Cell_, _135_(4), 738–748. https://doi.org/10.1016/j.cell.2008.10.028

Hermesdorf, M., Wulms, N., Maceski, A., Leppert, D., Benkert, P., Wiendl, H., Kuhle, J., & Berger, K. (2023). Serum neurofilament light and white matter characteristics in the general population: A longitudinal analysis. _Geroscience._, _46_, 463–472. https://doi.org/10.1007/s11357-023-00846-x

Herz, J., & Strickland, D. K. (2001). LRP: A multifunctional scavenger and signaling receptor. _The Journal of Clinical Investigation_, _108_(6), 779–784. https://doi.org/10.1172/JCI13992

Hess, D. M., Scott, M. O., Potluri, S., Pitts, E. V., Cisterni, C., & Balice-Gordon, R. J. (2007). Localization of TrkC to Schwann cells and effects of neurotrophin-3 signaling at neuromuscular synapses. _The Journal of Comparative Neurology_, _501_(4), 465–482. https://doi.org/10.1002/cne.21163

Jessen, K. R., & Mirsky, R. (2016). The repair Schwann cell and its function in regenerating nerves. _The Journal of Physiology_, _594_(13), 3521–3531. https://doi.org/10.1113/JP270874

Jessen, K. R., & Mirsky, R. (2019). The success and failure of the Schwann cell response to nerve injury. _Frontiers in Cellular Neuroscience_, _13_(33), 2019. https://doi.org/10.3389/fncel.2019.00033.eCollection

Khodabakhsh, P., Pournajaf, S., Mohaghegh Shalmani, L., Ahmadiani, A., & Dargahi, L. (2021). Insulin promotes Schwann-like cell differentiation of rat epidermal neural crest stem cells. _Molecular Neurobiology_, _58_(10), 5327–5337. https://doi.org/10.1007/s12035-021-02423-9

Kim, H. A., Pomeroy, S. L., Whoriskey, W., Pawlitzky, I., Benowitz, L. I., Sicinski, P., Stiles, C. D., & Roberts, T. M. (2000). A developmentally regulated switch directs regenerative growth of Schwann cells through cyclin D1. _Neuron_, _26_(2), 405–416. https://doi.org/10.1016/s0896-6273(00)81173-3

Koch, N., Koch, D., Krueger, S., Tröger, J., Sabanov, V., Ahmed, T., McMillan, L. E., Wolf, D., Montag, D., Kessels, M. M., Balschun, D., & Qualmann, B. (2020). Syndapin I loss-of-function in mice leads to schizophrenia-like symptoms. _Cerebral Cortex_, _30_(8), 4306–4324. https://doi.org/10.1093/cercor/bhaa013

Law, C. W., Chen, Y., Shi, W., & Smyth, G. K. (2014). Voom: Precision weights unlock linear model analysis tools for RNA-seq read counts. _Genome Biology_, _15_(2), R29. https://doi.org/10.1186/gb-2014-15-2-r29

Lehmann, H. C., & Höke, A. (2010). Schwann cells as a therapeutic target for peripheral neuropathies. _CNS & Neurological Disorders Drug Targets_, _9_(6), 801–806. https://doi.org/10.2174/187152710793237412

Li, B., & Dewey, C. N. (2011). RSEM: Accurate transcript quantification from RNA-seq data with or without a reference genome. _BMC Bioinformatics_, _12_, 323. https://doi.org/10.1186/1471-2105-12-323

Liu, Y., Lv, K., Li, Z., Yu, A. C., Chen, J., & Teng, J. (2012). PACSIN1, a tau-interacting protein, regulates axonal elongation and branching by

facilitating microtubule instability. *The Journal of Biological Chemistry*, 287(47), 39911–39924. https://doi.org/10.1074/jbc.M112.403451

Luo, L., Wall, A., Tong, S. J., Hung, Y., Xiao, Z., Tarique, A. A., et al. (2018). TLR crosstalk activates LRP1 to recruit Rab8a and PI3Kγ for suppression of inflammatory responses. *Cell Reports*, 24(11), P3033–P3044.

Mantuano, E., Azmoon, P., Banki, M. A., Gunner, C. B., & Gonias, S. L. (2022). The LRP1/CD91 ligands, tissue-type plasminogen activator, α2-macroglobulin, and soluble cellular prion protein have distinct co-receptor requirements for activation of cell signaling. *Scientific Reports*, 21(1), 17594. https://doi.org/10.1038/s41598-022-22498-1

Mantuano, E., Gonias, S. L., & Campana, W. M. (2010). Low density lipoprotein receptor related protein (LRP1) regulates Rac1 and RhoA reciprocally to control Schwan cell adhesion and migration. *The Journal of Biological Chemistry*, 825, 14259–14266.

Mantuano, E., Henry, K., Yamauchi, T., Hiramatsu, N., Yamauchi, K., Orita, S., Takahashi, K., Lin, J. H., Gonias, S. L., & Campana, W. M. (2011). The unfolded protein response is a major mechanism by which LRP1 regulates Schwann cell survival after injury. *The Journal of Neuroscience*, 31, 13376–13385. https://doi.org/10.1074/jbc.M109.085126

Mantuano, E., Inoue, G., Li, X., Takahashi, K., Gaultier, A., Gonias, S. L., & Campana, W. M. (2008). The hemopexin domain of matrix metalloproteinase-9 activates cell signaling and promotes migration of schwann cells by binding to low-density lipoprotein receptor-related protein. *The Journal of Neuroscience*, 28, 11571–11582. https://doi.org/10.1523/JNEUROSCI.3053-08.2008

Mantuano, E., Lam, M. S., & Gonias, S. L. (2013). LRP1 assembles unique co-receptor systems to initiate cell signaling in response to tissue-type plasminogen activator and myelin-associated glycoprotein. *The Journal of Biological Chemistry*, 288(47), 34009–34018. https://doi.org/10.1074/jbc.M113.509133

Mantuano, E., Lam, M. S., Shibayama, M., Campana, W. M., & Gonias, S. L. (2015). The NMDA receptor functions independently and as an LRP1 co-receptor to promote Schwann cell survival and migration. *Journal of Cell Science*, 128(18), 3478–3488. https://doi.org/10.1242/jcs.173765

Martin, M. G., Perga, S., Trovò, L., Rasola, A., Holm, P., Rantamäki, T., Harkany, T., Castrén, E., Chiara, F., & Dotti, C. G. (2008). Cholesterol loss enhances TrkB signaling in hippocampal neurons aging in vitro. *Molecular Biology of the Cell*, 19(5), 2101–2112. https://doi.org/10.1091/mbc.e07-09-0897

Mattei, V., Manganelli, V., Martellucci, S., Capozzi, A., Mantunao, E., Longo, A., et al. (2020). A multimolecular signaling complex including PrP^c and LRP1 is strictly dependent on lipid rafts and is essential for the function of tissue plasminogen activator. *Journal of Neurochemistry*, 152(4), 468–481. https://doi.org/10.1111/jnc.14891

May, P., Rohlmann, A., Bock, H. H., Zurhove, K., Marth, J. D., Schomburg, E. D., Schomburg, E. D., Noebels, J. L., Beffert, U., Sweatt, J. D., Weeber, E. J., & Herz, J. (2004). neurona8872-83l LRP1 functionally associates with post synaptic proteins and is required for normal motor function in mice. *Molecular and Cellular Biology*, 24(20), 8872–8883. https://doi.org/10.1128/MCB.24.20.8872-8883.2004

Mikhailenko, I., Battey, F. D., Migliorini, M., Ruiz, J. F., Argraves, K., Moayeri, M., & Strickland, D. K. (2001). Recognition of alpha 2-macroglobulin by the low density lipoprotein receptor-related protein requires the cooperation of two ligand binding cluster regions. *The Journal of Biological Chemistry*, 276(42), 39484–39491. https://doi.org/10.1074/jbc.M104382200

Min, Q., Parkinson, D. B., & Dun, X. P. (2021). Migrating Schwann cells direct axon regeneration within the peripheral nerve bridge. *Glia*, 69(2), 235–254. https://doi.org/10.1002/glia.23892

Moreno, P., Fexova, S., George, N., Manning, J. R., Miao, Z., Mohammed, S., Muñoz-Pomer, A., Fullgrabe, A., Bi, Y., Bush, N., Iqbal, H., Kumbham, U., Solovyev, A., Zhao, L., Prakash, A., García-Seisdedos, D., Kundu, D. J., Wang, S., Walzer, M., … Papatheodorou, I. (2022). Expression atlas update: Gene and protein expression in multiple species. *Nucleic Acids Research*, 50(D1), D129–D140. https://doi.org/10.1093/nar/gkab1030

Neels, J. G., van Den Berg, B. M., Lookene, A., Olivecrona, G., Pannekoek, H., & van Zonneveld, A. J. (1999). The second and fourth cluster of class a cysteine-rich repeats of the low density lipoprotein receptor-related protein share ligand-binding properties. *The Journal of Biological Chemistry*, 274(44), 31305–31311. https://doi.org/10.1074/jbc.274.44.31305

Nguyen, D. H., Catling, A. D., Webb, D. J., Sankovic, M., Walker, L. A., Somlyo, A. V., et al. (1999). Myosin light chain kinase functions downstream of Ras/ERK to promote migration of urokinase-type plasminogen activator-stimulated cells in an integrin-selective manner. *The Journal of Cell Biology*, 146(1), 149–164. https://doi.org/10.1083/jcb.146.1.149

Nikam, S. S., Tennekoon, G. I., Christy, B. A., Yoshino, J. E., & Rutkowski, J. L. (1995). The zinc finger transcription factor Zif268/Egr-1 is essential for Schwann cell expression of the p75 NGF receptor. *Molecular and Cellular Neurosciences*, 6(4), 337–348. https://doi.org/10.1006/mcne.1995.1026

Orita, S., Henry, K., Mantuano, E., Yamauchi, K., De Corato, A., Ishikawa, T., et al. (2013). Schwann cell LRP1 regulates remak bundle ultrastructure and axonal interactions to prevent neuropathic pain. *The Journal of Neuroscience*, 33, 5590–5602. https://doi.org/10.1523/JNEUROSCI.3342-12.2013

Painter, M. W., Brosius, L. A., Cheng, Y. C., Latremoliere, A., Duong, K., Miller, C. M., et al. (2014). Diminished Schwann cell repair responses underlie age-associated impaired axonal regeneration. *Neuron*, 83(2), 331–343. https://doi.org/10.1016/j.neuron.2014.06.016

Paulus, W., Baur, I., Dours-Zimmermann, M. T., & Zimmermann, D. R. (1996). Differential expression of versican isoforms in brain tumors. *Journal of Neuropathology and Experimental Neurology*, 55(5), 528–533. https://doi.org/10.1097/00005072-199605000-00005

Poplawski, G. H. D., Lie, R., Hunt, M., Kumamaru, H., Kawaguchi, R., Lu, P., Schäfer, M. K. E., Woodruff, G., Robinson, J., Canete, P., Dulin, J. N., Geoffroy, C. G., Menzel, L., Zheng, B., Coppola, G., & Tuszynski, M. H. (2018). Adult rat myelin enhances axonal outgrowth from neural stem cells. *Science Translational Medicine*, 10(442), eaal2563. https://doi.org/10.1126/scitranslmed.aal2563

Puehringer, D., Orel, N., Lüningschrör, P., Subramanian, N., Herrmann, T., Chao, M. V., & Sendtner, M. (2013). EGF transactivation of Trk receptors regulates the migration of newborn cortical neurons. *Nature Neuroscience*, 16(4), 407–415. https://doi.org/10.1038/nn.3333

Qiu, Z., Strickland, D. K., Hyman, B. T., & Rebeck, G. W. (2002). Alpha 2-macroglobulin exposure reduces calcium responses to N-methyl-D-aspartate via low density lipoprotein receptor-related protein in cultured hippocampal neurons. *The Journal of Biological Chemistry*, 277(17), 14458–14466. https://doi.org/10.1074/jbc.M112066200

Qualmann, B., & Kelly, R. B. (2000). Syndapin isoforms participate in receptor-mediated endocytosis and Actin organization. *The Journal of Cell Biology*, 148(5), 1047–1062. https://doi.org/10.1083/jcb.148.5.1047

Ritchie, M. E., Phipson, B., Wu, D., Hu, Y., Law, C. W., Shi, W., & Smyth, G. K. (2015). Limma powers differential expression analyses for RNA-sequencing and microarray studies. *Nucleic Acids Research*, 43(7), e47. https://doi.org/10.1093/nar/gkv007

Robinson, M. D., McCarthy, D. J., & Smyth, G. K. (2010). edgeR: A Bioconductor package for differential expression analysis of digital gene expression data. *Bioinformatics*, 26(1), 139–140. https://doi.org/10.1093/bioinformatics/btp616

Rohrbach, S., Li, L., Novoyatleva, T., Niemann, B., Knapp, F., Molenda, N., & Schulz, R. (2021). Impact of PCSK9 on CTRP9-induced metabolic effects in adult rat cardiomyocytes. *Frontiers in Physiology*, 12, 593862. https://doi.org/10.3389/fphys.2021.593862

Rusanescu, G., Qi, H., Thomas, S. M., Brugge, J. S., & Halegoua, S. (1995). Calcium influx induces neurite growth through a Src-Ras signaling

cassette. *Neuron*, *15*(6), 1415–1425. https://doi.org/10.1016/0896-6273(95)90019-5

Sadri, M., Hirosawa, N., Le, J., Romero, H., Martellucci, S., Kwon, H. J., et al. (2022). Tumor necrosis factor receptor-1 is selectively sequestered into Schwann cell extracellular vesicles where it functions as a TNFα decoy. *Glia*, *70*(2), 256–272. https://doi.org/10.1002/glia.24098

Sanz, E., Yang, L., Su, T., Morris, D. R., McKnight, G. S., & Amieux, P. S. (2009). Cell-type-specific isolation of ribosome-associated mRNA from complex tissues. *Proceedings of the National Academy of Sciences of the United States of America*, *106*(33), 13939–13944. https://doi.org/10.1073/pnas.0907143106

Schael, S., Nüchel, J., Müller, S., Petermann, P., Kormann, J., Pérez-Otaño, I., Martínez, S. M., Paulsson, M., & Plomann, M. (2013). Casein kinase 2 phosphorylation of protein kinase C and casein kinase 2 substrate in neurons (PACSIN) 1 protein regulates neuronal spine formation. *The Journal of Biological Chemistry*, *288*(13), 9303–9312. https://doi.org/10.1074/jbc.M113.461293

Schecterson, L. C., & Bothwell, M. (2010). Neurotrophin receptors: Old friends with new partners. *Developmental Neurobiology*, *70*(5), 332–338. https://doi.org/10.1002/dneu.20767

Shi, Y., Mantuano, E., Inoue, G., Campana, W. M., & Gonias, S. L. (2009). Ligand binding to LRP1 transactivates Trk receptors by a Src family kinase-dependent pathway. *Science Signaling*, *2*(68), ra18. https://doi.org/10.1126/scisignal.2000188

Stiles, T. L., Dickendesher, T. L., Gaultier, A., Fernandez-Castaneda, A., Mantuano, E., Giger, R. J., & Gonias, S. L. (2013). LDL receptor-related protein-1 is a sialic-acid-independent receptor for myelin-associated glycoprotein that functions in neurite outgrowth inhibition by MAG and CNS myelin. *Journal of Cell Science*, *126*(Pt 1), 209–220. https://doi.org/10.1242/jcs.113191

Strickland, D. K., Gonias, S. L., & Argraves, W. S. (2002). Diverse roles for the LDL receptor family. *Trends in Endocrinology and Metabolism*, *13*(2), 66–74. https://doi.org/10.1016/s1043-2760(01)00526-4

Syed, N., Reddy, K., Yang, D. P., Taveggia, C., Salzer, J. L., Maurel, P., & Kim, H. A. (2010). Soluble neuregulin-1 has bifunctional, concentration-dependent effects on Schwann cell myelination. *The Journal of Neuroscience*, *30*(17), 6122–6131. https://doi.org/10.1523/JNEUROSCI.1681-09.2010

Taylor, D. R., & Hooper, N. M. (2007). The low density lipoprotein receptor-related protein 1 (LRP1) mediates the endocytosis of the cellular prior protein. *The Biochemical Journal*, *402*(1), 17–23. https://doi.org/10.1042/BJ20061736

Thornhill, P. B., Cohn, J. B., Drury, G., Stanford, W. L., Bernstein, A., & Desbarats, J. (2007). A proteomic screen reveals novel Fas ligand interacting proteins within nervous system Schwann cells. *FEBS Letters*, *581*(23), 4455–4462. https://doi.org/10.1016/j.febslet.2007.08.025

Topilko, P., Levi, G., Merlo, G., Mantero, S., Desmarquet, C., Mancardi, G., & Charnay, P. (1997). Differential regulation of the zinc finger genes Krox-20 and Krox-24 (Egr-1) suggests antagonistic roles in Schwann cells. *Journal of Neuroscience Research*, *50*(5), 702–712. https://doi.org/10.1002/(SICI)1097-4547(19971201)50:5<702::AID-JNR7>3.0.CO;2-L

Verschueren, E., Von Dollen, J., Cimermancic, P., Gulbahce, N., Sali, A., & Krogan, N. J. (2015). Scoring large-scale affinity purification mass spectrometry datasets with MiST. *Current Protocols in Bioinformatics*, *49*, 8.19.1–8.19.16. https://doi.org/10.1002/0471250953.bi0819s49

Wang, Z., Martellucci, S., Van Enoo, A., Austin, D., Gelber, C., & Campana, W. M. (2022). α1-antitrypsin derived SP16 peptide demonstrates efficacy in rodent models of acute and neuropathic pain. *The FASEB Journal*, *36*(1), e22093. https://doi.org/10.1096/fj.202101031RR

Warren, P. M., Andrews, M. R., Smith, M., Bartus, K., Bradbury, E. J., Verhaagen, J., Fawcett, J. W., & Kwok, J. C. F. (2020). Secretion of a mammalian chondroitinase ABC aids glial integration at PNS/CNS boundaries. *Scientific Reports*, *10*(1), 11262. https://doi.org/10.1038/s41598-020-67526-0

Widagdo, J., Fang, H., Jang, S. E., & Anggono, V. (2016). PACSIN1 regulates the dynamics of AMPA receptor trafficking. *Scientific Reports*, *6*, 31070. https://doi.org/10.1038/srep31070

Yamauchi, J., Chan, J. R., & Shooter, E. M. (2003). Neurotrophin 3 activation of TrkC induces Schwann cell migration through the c-Jun N-terminal kinase pathway. *Proceedings of the National Academy of Sciences of the United States of America*, *100*(24), 14421–14426. https://doi.org/10.1073/pnas.2336152100

Yang, D. P., Zhang, D. P., Mak, K. S., Bonder, D. E., Pomeroy, S. L., & Kim, H. A. (2008). Schwann cell proliferation during Wallerian degeneration is not necessary for regeneration and remyelination of the peripheral nerves: Axon-dependent removal of newly generated Schwann cells by apoptosis. *Molecular and Cellular Neurosciences*, *38*(1), 80–88. https://doi.org/10.1016/j.mcn.2008.01.017

Ye, Y., Li, X., Zhang, Y., Shen, Z., & Yang, J. (2016). Androgen modulates functions of endothelial progenitor cells through activated Egr1 signaling. *Stem Cells International*, *2016*, 7057894. https://doi.org/10.1155/2016/7057894

Yoon, C., Van Niekerk, E. A., Henry, K., Ishikawa, T., Orita, S., Tuszynski, M. H., & Campana, W. M. (2013). Low-density lipoprotein receptor-related protein 1 (LRP1)-dependent cell signaling promotes axonal regeneration. *The Journal of Biological Chemistry*, *288*(37), 26557–26568. https://doi.org/10.1074/jbc.M113.478552

Yun, B., Anderegg, A., Menichella, D., Wrabetz, L., Feltri, M. L., & Awatramani, R. (2010). MicroRNA-deficient Schwann cells display congenital hypomyelination. *The Journal of Neuroscience*, *30*(22), 7722–7728. https://doi.org/10.1523/JNEUROSCI.0876-10.2010

SUPPORTING INFORMATION

Additional supporting information can be found online in the Supporting Information section at the end of this article.